Scientific Report 2007

Institute for Energy Research-
Safety Research and Reactor Technology (IEF-6)

Safety Research for Nuclear Reactors

Contents:

Calculation of the Spatial Neutron and Prompt Gamma-Ray Heating Rates in the Components of an HTR with a Central Column

H. Brockmann and A. Kuhr

Institute of Energy Research (IEF-6), Forschungszentrum Jülich, Germany
Corresponding author: h.brockmann@fz-juelich.de

Abstract - The further development of the two-group reactor dynamics code TINTE into the multigroup version MGT and the use of a central column in some recent HTR designs required a re-examination of the treatment of the non-local heat sources. For this purpose, the spatial neutron and prompt gamma-ray heating rates in the components of a typical HTR design with a central column were calculated on the basis of the transport theory. The calculations were performed by the discrete ordinates transport code XSDRNPM in the P_3-S_{16} approximation. The neutron and gamma-ray cross sections were taken from the VITAMIN B-6 library. The information on the heat deposition in the components of an HTR thus obtained was transferred to the new MGT code in order to update the previous procedure for treating the non-local heat sources in the presence of a central column and to adjust it to the new circumstances of a multigroup code.

Introduction

A non-negligible amount of the energy released in the nuclear fission process is not deposited at the location of its emergence but - after a certain number of interactions - at a distance from it. This effect is treated in the reactor dynamics code TINTE [1] by a procedure that in the past was tested by explicit coupled neutron gamma-ray transport calculations. Due to the extension of the two-group TINTE code to the multigroup code MGT [2] and the use of a central column in some recent HTR designs it became necessary to re-examine the method for treating the non-local heat sources and to adapt it to the new circumstances. For this purpose, detailed calculations of the spatial neutron and prompt gamma-ray power density distributions in the core and the outer components of a typical HTR with a central column were made on the basis of the transport theory.

Calculation Method and Nuclear Data

The transport calculations were performed in the power maximum of the reactor using the discrete ordinates transport code XSDRNPM, a module of the SCALE 5 code system [3]. The number of energy groups used in the transport calculations was 199 (with 36 thermal groups) for the neutrons and 42 for the gamma-rays. The calculations were made in the P_3-S_{16} approximation. The multigroup neutron and gamma-ray cross sections and the KERMA factors[a] were taken from the VITAMIN B-6 library [4]. The gamma-ray KERMA factors on the library had to be corrected due to an inconsistency to which the original version was subject.

The self-shielding of the resonance cross sections was performed by the use of the Bondarenko method and the BONAMI module of the SCALE 5 system. The nuclide concentrations required for this purpose were taken from the design calculations for the equilibrium core, which were made by the reactor analysis code system V.S.O.P. [5], and the geometry was treated as homogeneous.

Determination of the Neutron Fission Source in the Core

The required space- and energy-dependent source distribution of the fission neutrons in the reactor core was also determined by the use of the results obtained in the design calculations for the equilibrium core. The V.S.O.P. fission rate distribution was interpolated and re-calculated for a fine mesh used in the transport calculations. The energy distribution of the fission neutrons was determined by the ICE-II module of the

[a] KERMA: Kinetic Energy Released in Matter.

AMPX77 code system [6] on the basis of a typical HTR core composition.

Results and Discussion

The neutron transport calculation in the core region is not as accurate as the detailed reactor design calculation. Reasons for this are, for example, that neither the neutron streaming effect in the HTR pebble bed core nor the double heterogeneity of the fuel is considered. In order to get an idea of the accuracy of the transport calculation in the core region, the neutron fluxes at the boundaries between the core and the central column and between the core and the outer reflector obtained by the two codes are compared in Table I and Table II.

It is seen from the tables that the deviations between the fluxes at the inner and outer core boundary

Table I
Neutron Fluxes at the Boundary between the Core and Central Column at the Power Maximum.

Energy Range	V.S.O.P.	XSDRN	Δ [%]
10 MeV – 0.1 MeV	$5.009 \cdot 10^{13}$	$4.844 \cdot 10^{13}$	3.34
0.1 MeV – 130 eV	$7.372 \cdot 10^{13}$	$7.364 \cdot 10^{13}$	0.11
130 eV – 1.86 eV	$3.876 \cdot 10^{13}$	$3.941 \cdot 10^{13}$	-1.67
1.86 eV – 10^{-5} eV	$2.194 \cdot 10^{14}$	$2.118 \cdot 10^{14}$	3.52

obtained by the two calculation methods are lower than 5 %. Thus, the agreement between the results is sufficiently accurate with respect to the problem to be analyzed.

Table II
Neutron Fluxes at the Boundary between the Core and the Outer Reflector at the Power Maximum.

Energy Range	V.S.O.P.	XSDRN	Δ [%]
10 MeV – 0.1 MeV	$3.995 \cdot 10^{13}$	$3.801 \cdot 10^{13}$	4.98
0.1 MeV – 130 eV	$5.877 \cdot 10^{13}$	$5.748 \cdot 10^{13}$	2.21
130 eV – 1.86 eV	$3.077 \cdot 10^{13}$	$3.070 \cdot 10^{13}$	0.24
1.86 eV – 10^{-5} eV	$1.633 \cdot 10^{14}$	$1.635 \cdot 10^{14}$	-0.15

The nuclear heating rates were calculated in the reactor core, the inner and outer reflector regions, the core barrel, the reactor vessel, and the wall of the reactor cell. The results of the heating calculations in the reflector regions are of main interest concerning the problem of the treatment of the non-local heat sources in the TINTE or MGT code. They are shown in Figs. 1 and 2.

Fig. 1 gives the neutron and gamma-ray heating rates in the central column as a function of the distance from the core center. The inner part up to a distance of 10 cm is made up of a cooling channel by means of which the heat generated in the central column is removed. It is seen that the gamma-ray heating makes the major contribution to the total heating. While the neutron heating rate is of the same order of magnitude in the vicinity of the core boundary, it is more than one order of magnitude lower than the gamma-ray heating in the inner part of the central column. The discontinuities of the heating rates at the locations 81 cm and 92 cm are due to a change in the material properties in the region in between which contains the bore holes for the KLAK system[b].

Fig. 2 gives the neutron and gamma-ray heating rates in the outer reflector regions as a function of the distance from the core center.

[b] KLAK: Kleine Absorber-Kugeln (English: Small Absorber Spheres).

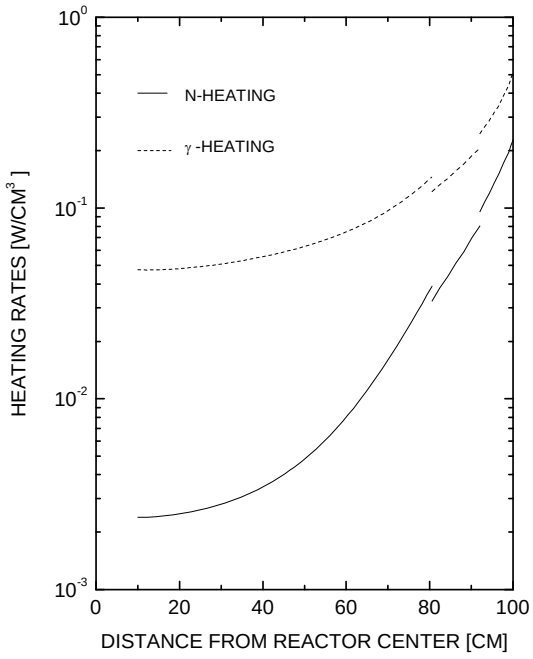

Fig. 1 Neutron and prompt gamma-ray heating rates in the central column at the power maximum as a function of the distance from the center of the reactor core.

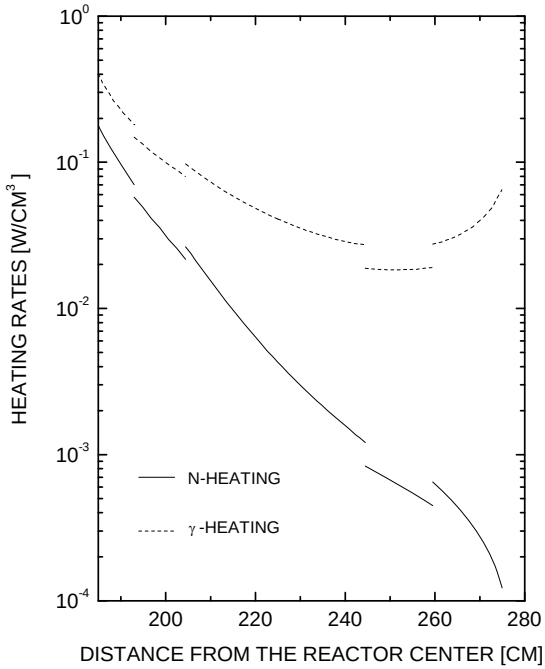

Fig. 2 Neutron and prompt gamma-ray heating rates in the outer reflector at the power maximum as a function of the distance from the center of the reactor core.

With increasing distance from the core the contribution of the neutron heating becomes negligible compared to the gamma-ray heating. The discontinuities here occur at the locations 193 cm and 205 cm, which enclose the region containing the absorber rods and at the locations 245 cm and 260 cm, which enclose the region through which the cold gas is re-circulated. The increase of the gamma-ray heating rate in the outer reflector region is due to the capture gamma-rays, which are generated in the core barrel by neutron capture processes and are back-scattered into the reflector.

The information on the neutron and gamma-ray heating rates in the inner and outer reflector regions thus obtained for a typical HTR design with a central column was subsequently used in order to update the method for treating the non-local heat sources for this situation in the reactor dynamics code TINTE and to re-adjust the method in the transition from the two-group TINTE code to the multigroup code MGT.

References

[1] H. Gerwin, Das zweidimensionale Reaktordynamikprogramm TINTE Teil 1: Grundlagen und Lösungsverfahren, Jül-2165, Kernforschungsanlage Jülich (1987).

[2] H. Gerwin, personal communication.

[3] SCALE: A Modular Code System for Performing Standardized Computer Analyses for Licensing Evaluation, ORNL/TM-2005/39, Version 5, Oak Ridge National Laboratory (2005).

[4] J. E. White et al, VITAMIN B-6: A Fine-Group Cross Section Library Based on ENDF/B-VI for Radiation Transport Applications, Proceedings of the International Conference on Nuclear Data for Science and Technology, Gatlinburg, Tennessee, pp.733-736 (1994).

[5] H. J. Rütten, K. A. Haas, H. Brockmann and W. Scherer, V.S.O.P.(99/05) Computer Code System, Jül-4189, Forschungszentrum Jülich (2005).

[6] N. M. Greene et al., AMPX77: A Modular Code System for Generating Coupled Multigroup Neutron Gamma Cross Section Libraries, ORNL/CSD/TM-283, Oak Ridge National Laboratory (1992).

Comparison of Multi-Group Energy Models for a PBMR-like HTR in Transient Operating Conditions

C. Druska, St. Kasselmann, A. Lauer

Institute for Energy Research (IEF-6), Forschungszentrum Jülich
Corresponding author: S.Kasselmann@fz-juelich.de

The energy spectra of fast and thermal neutrons from fission reactions so far were modelled by two broad energy groups. Present demands for increased numerical accuracy led to the question of how precise the 2-group approximation is compared to a multi-group model. Therefore a new simulation program has recently been developed which is able to handle up to 43 energy groups. Furthermore, an internal spectrum calculation for the cross-section calculation can be performed for each time step and location within the reactor. In this study the multi-group energy models are compared to former calculations with only two energy groups. Different scenarios (normal operation and design-basis accidents) have been defined for a PBMR-like high temperature reactor (HTR) design. The effect of an increasing number of energy groups on safety-related parameters like the fuel and coolant temperature, the nuclear heat source or the xenon concentration is studied. Different ways of calculating the material cross-sections are compared as well.

Incentives and scope of the research

The correct treatment of neutron sources, neutron scattering and neutron absorption in terms of diffusion theory is a crucial point in simulating the dynamical behaviour of a nuclear reactor. The calculation of neutron fluxes for a non-trivial core geometry composed of a large variety of materials using more than 2 energy groups can only be solved numerically and iteratively. An introduction to this topic can for example be found in [Ryd77], [Nai79] or [Sta07].

To simulate the steady-state and transient behaviour of a gas cooled high temperature reactor as the one shown in fig. 1, the two-dimensional reactor dynamics code system TINTE (TIme dependent Nucleonics and TEmperatures) has been developed in the past [Ger87a, Ger87b]. Since then it has been widely used in several HTR projects worldwide. One limitation of TINTE is that the neutron energy spectrum is modelled by only 2 energy groups, namely a thermal and a fast group. In addition, the cross-sections for the various core materials are not calculated for each single time step, but determined by linear and polynomial fit interpolations of a table, which is created just once before the main simulation. Therefore a multi-group derivative of TINTE called MGT (Multi-Group TINTE) has been developed, which is able to handle up to 43 energy groups [Lau07]. Further-more, an internal spectrum calculation for the cross-section calculation can be performed for each time step and location within the reactor. The multi-group diffusion equations in MGT are solved by an iterative leakage method. The integrated spectral code MUPO calculates the critical neutron spectrum for a homogeneous reactor core by using up to 43 energy groups. This spectrum is then used to evaluate condensed macroscopic region cross-sections.

In addition to the comparison of different energy group models, different ways of calculating the material cross-sections for fission, absorption, scattering etc. are compared. These three methods are:

- Internal spectrum calculations (spec.),
- Linear interpolation from table (tab.),
- Polynomial interpolation func. (pol.).

While the first method is computationally intensive compared to the other strategies but yields the highest precision, the second method is quite fast and can be applied for all models of up to 43 (broad) energy groups. Due to convergence problems the third method was found to be only applica-

ble for 10 energy groups or less in the case of steady-state full power operation and for only 2 groups in the case of the accident scenarios.
For a nuclear fission reactor the following parameters are of major importance: The thermal and fast neutron flux, the heat source (power density), the maximum fuel kernel temperature, the coolant temperature, the temperature of the surrounding infrastructure and the xenon concentration. For each of those parameters the deviations between the multi-group-models and the 2-group model have been studied at different locations within the reactor and for three different scenarios (operating conditions):

- **Steady State Full Power (SSFP)**: The reactor is operated at a constant thermal power of about 400 MWth. This scenario reflects the normal operation of the reactor and, in addition, is the starting point for further non-stationary (transient) simulations.

- **Total Withdrawal of Control Rods (TWCR):**
  This is a design-basis accident. Here the rod banks located in the side reflector are withdrawn from their nominal position at a normal speed of 1 cm/s. Details about the rod movement simulation can be found in [Lau04]. At the same time, the helium gas turbine is expected to stay operational, so the coolant mass flow and the coolant pressure at the outlet is intentionally kept constant.

- **TWCR + DLOFC:**
  In the third scenario, the TWCR is followed by a depressurization and total loss of coolant (DLOFC). This may be caused by a breach or rupture of the main cooling pipe or any other kind of leakage in the reactor vessel. It is further assumed that no air ingress takes place. Since the heat removal then mainly depends on the effective conductivity of the core, this event is also known as a conduction heat-up.

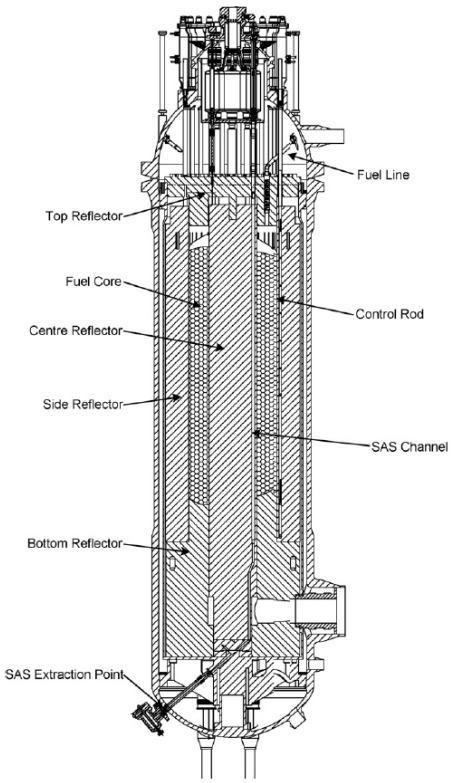

Fig. 1: Vertical cross-section schematic of a PBMR-like reactor unit [Pbm07].

25 representative locations within the reactor were chosen which are interesting from the physics point of view. In the radial (r) direction they are:

- the centre reflector,
- the transition between the centre reflector and the pebble bed,
- the radial centre of the pebble bed,
- the transition between the pebble bed and the side reflector,
- the side reflector itself.

Five points were also chosen for the axial (z) direction:

- the top reflector,
- the point where the thermal flux reaches half of its maximum,
- the point where the thermal flux has its maximum slope,
- the point of the maximum thermal flux,
- the point where the flux decreases to half of its maximum,
- the bottom reflector.

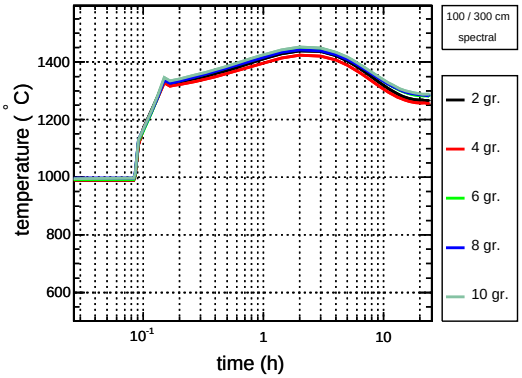

Fig. 2: Temporal evolution of the maxi-mum kernel temperature at r=100cm (transition core/side reflector) and z=300cm (thermal flux peak) for different energy group calculations (logarithmic scale) in the TWCR scenario.

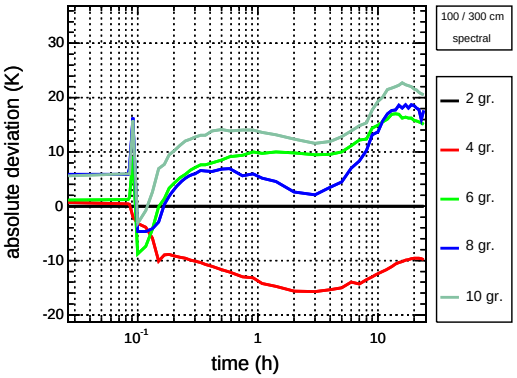

Fig. 3: Absolute deviation of the maximum kernel temperature at r=100cm (transition core/side reflector) and z=300cm (thermal flux peak) between different energy group calculations (logarithmic scale).

Results and conclusions

At each point the time-dependent absolute and relative deviations in the r/z plane between the different models were studied. It was found that there is very good agreement between the results provided by TINTE and MGT in the case of two energy groups. The usage of multi-group energy models leads to significant but not unexpected deviations.

As an example fig. 2 shows the temporal evolution of the maximum kernel temperature at r=100 cm and z=300 cm on a logarithmic time scale. This corresponds to the upper third of the core between the pebble bed and the centre reflector. As can be seen, the scenario starts with the state of full power operation. Afterwards the withdrawal of the control rods begins for about four minutes leading to a significant increase of the kernel temperature from 1000°C to about 1350°C. A global maximum temperature of 1430°C is reached 2 hours after the beginning of the accident.

From that time on, the temperature decreases again and converges to about 1250 °C after several hours. In the steady-state phase, a deviation of about 6K exists between the simulation using 2/4/6 and 8/10 broad energy groups (cf. fig. 3). Larger discrepancies emerge in the second (transient) phase of the scenario, especially after a few hours when the temperature decreases again. The maximum deviation from the 2-group calculation is about 23K for the 10-group model. Obviously the 6-,8- and 10-group calculations show slightly higher temperatures, and only the 4-group calculation leads to lower deviations which may result from the condensation of the 43 fine energy groups to one thermal and three fast (broad) energy groups (relation is 1:3 in contrast to 1:1 in all other cases).

As can be seen from the case of 4 energy groups, the parameters may be very sensitive to the condensation of fine groups to broad groups. This may lead to a significantly different shape for some of the studied parameters. A comparison with the other models should therefore be regarded with caution. Future studies will have to investigate this aspect in detail.

Under the assumption that the highest number of energy groups in combination with the spectral method of cross-section calculation yields the highest simulation precision, the results for the TWCR for example scenario can be summarized as follows when comparing 10 to 2 energy groups:

- The parameter deviations for non-stationary operating conditions are

higher than for the steady-state scenario as expected.

- The maximum fuel kernel temperature increases by at most 1.4% (spatial mean of pebble bed). The peak deviation found in a small area is 5.1%.

- The nuclear heat source increases by at most 1.3% (spatial mean of pebble bed). The peak deviation found in a small area is 14.6%.

- The xenon concentration increases by at most 0.5% (spatial mean of pebble bed). The peak deviation found in a small area is 6.1%.

There are thus deviations between the different group models for the space- as well as the time-dependent parameters on a percent level. This shows the necessity of cross-checking simulations performed with 2 neutron energy groups with multi-group energy models.
It has been found that for the studied scenarios the use of up to 8 energy groups is a good trade-off between precision calculations and a tolerable amount of computing time.

On the other hand, some calculations revealed larger deviations between different cross-section methods than between different group models using the same cross-section calculation. The optimum number of energy groups therefore depends on the scenario and the parameter of interest.

Outlook

In this study a first attempt was made to compare different energy group models. One of the next steps is the determination of an optimal splitting of the neutron energy spectrum into groups of energy intervals with respect to the fuel and material characteristics (e.g. considering cross-section resonances). This might allow us to reduce the number of energy groups without a loss of precision. In addition, systematic uncertainties have to be checked (e.g. the influence of the grid granularity or the cross-section determination).

References

[Ger87a] HELMUT GERWIN. Das zweidimensionale Reaktordynamik-programm TINTE (Teil I). Kernforschungsanlage Jülich GmbH, 1987.

[Ger87b] HELMUT GERWIN. Das zweidimensionale Reaktordynamik-programm TINTE (Teil II). Kernforschungsanlage Jülich GmbH, 1987.

[Lau04] A. LAUER. TINTE User Manual Supplement: The Rod Motion Extension ROMO. Technical report, Forschungszentrum Jülich GmbH, 2004. ISR-IB-1/2004.

[Lau07] A. LAUER. MGT - A Multi-Energy Group Derivative of Tinte. Talk, IAEA Technical Meeting (Beijing 2007).

[Pbm07] Pieter J. Venter and Mark N. Mitchell. Integrated design approach of the pebble BeD modular reactor using models. Nuclear Engineering and Design 237 (2007) 1341–1353

[Nai79] YOSHITAKA NAITO. Development of a three-dimensional neutron diffusion code series by leakage iterative method. Technical report, Japan Atomic Energy Research Institute (JAERI), May 1979. NEACRP-L-207.

[Ryd77] ROGER A. RYDIN. Nuclear Reactor - Theory and Design. University Publications, Blacksburg, Virginia (USA), 1977.

[Sta07] M. STACEY. Nuclear Reactor Physics. WILEY-VCH Verlag GmbH & Co., Weinheim (Germany), 2007.

Dust retention during HTR pressure relief by water scrubbers

S. Jühe*, S. Struth

**Lehrstuhl für Reaktorsicherheit und –technik, RWTH Aachen, Germany*
Institut für Energieforschung (IEF-6), Forschungszentrum Jülich, Germany
Corresponding author: s.struth@fz-juelich.de

Abstract: Efforts have been made to calculate the pressure relief from an HTR through a water scrubber. Scrubbing of the gasses is recommended because of the mobilisation of contaminated dust particles form the primary circuit during pressure relief.
In cooperation with TU Darmstadt, the results of the calculations were used to develop a modular water scrubber for dust retention.

The latest goal of *des2neuFilter* calculations of HTR pressure relief was to determine the conditions of the gas flowing out of the reactor building in order to be able to design an appropriate filter system.
As shown in Figure 1, a primary circuit break with a hydraulic diameter of 230 *mm* will lead to very high mass flows out of the reactor building if the concept of a vented confinement is applied.

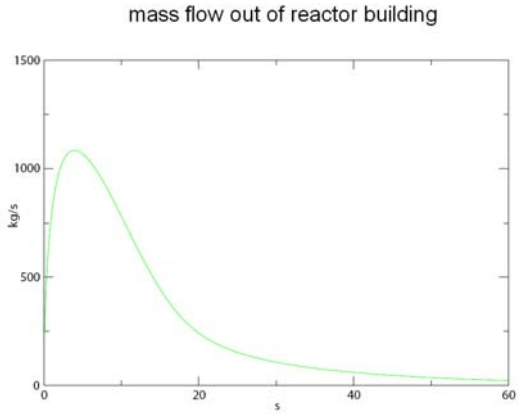

Fig.1 *Mass flow out of reactor building for a d_h=230 mm leak*

Current filtered venting systems for nuclear facilities were systematically studied to determine if they are suited for such an application. The main result was that most systems can only handle much lower mass flow rates. The most promising concept from the flow rate point of view is a simple water scrubber.

Ongoing experimental studies in cooperation with TU Darmstadt showed that fine dust can be retained to a high degree by a rather shallow water pool. Types of dust studied were dust from corrosion at the NAKOK-facility, dust from graphite abrasion from fuel handling and printer toner.
Dust retention has been demonstrated up to a mass flow rate of 0.5 *kg/s*; the reason for that limitation was not the scrubber itself, but the air blower supplying the air flow. The experimental scrubber with the blower is shown in Fig.2.

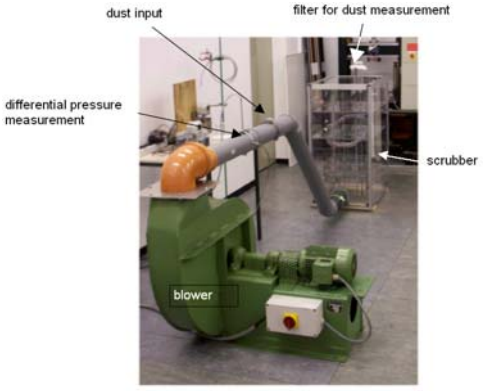

Fig.2 *Scrubber experiment* [1]

With a new blower installed, it will be possible to determine the maximal mass flow rate for sufficient dust retention. There will be further experiments with a modified scrubber unit in order to find an optimal configuration
With the data gathered from those experiments, it will be possible to integrate an empirically backed scrubber model into the existing pressure relief code *des2neuFilter*.

[1] J. Unger, *Untersuchung zur Abscheidung von Feinstäuben in einem Wasserbad,* Report, TU Darmstadt, 2007

Generation of Neutron Scattering Data for Various Moderator Materials to be Used in the Reactor Code System V.S.O.P.

H. Brockmann, K.A. Haas, H.J. Rütten

Institute of Energy Research (IEF-6), Forschungszentrum Jülich, Germany
Corresponding author: h.brockmann@fz-juelich.de

Abstract – In continuing the activities for updating the thermal scattering data used in the V.S.O.P. code system group averaged cross sections and scattering matrices were calculated at different temperatures for the moderators H-1 in H_2O and H-2 in D_2O on the basis of the ENDF/B-VI library and for the scatterers Be, Be in BeO and of BeO on the basis of the ENDF/B-VII library. The cross sections were generated by the use of the NJOY and AMPX77 processing codes and the 97 group structure of the THERMALIZATION library. In a first step, new 97 group transport cross sections were calculated on the basis of the new data by the use of the XSDRNPM module of the AMPX77 code system. The resulting transport cross sections were collapsed with a representative high temperature reactor spectrum to the 30 group structure of the THERMOS cross section library of the V.S.O.P. code system. It was started to update also the remaining thermal cross sections used in the V.S.O.P. code by converting the new cross section data given in the AMPX master library format into the format of the THERMALIZATION library. Furthermore, test calculations with the new cross section data were made in which the effect of the scattering matrices for bound-atom systems was compared with that of the scattering matrices for the free gas model.

Introduction

The activities for updating the thermal neutron cross section data on the basis of the ENDF/B-VI and ENDF/B-VII libraries [1] for the moderator materials given on the THERMALIZATION and on the THERMOS library [2]of the V.S.O.P. code system [3] were continued. In a first step, new thermal transport cross sections were calculated at different temperatures for the moderators H-1 in H_2O and H-2 in D_2O and for the scatterers Be, Be in BeO, and BeO. Furthermore, it was started to update the other one-dimensional group data and the thermal scattering matrices on the THERMALIZATION library and the THERMOS library of the V.S.O.P. code system as well. The procedure used for calculating and updating the new thermal data is given in the following. Within the scope of the update process test calculations with the new scattering data were made which are also described.

Calculation of the Thermal Transport Cross Sections

The group transport cross sections for the thermal neutrons (10^{-5} eV – 5 eV) were generated using the 97 energy group structure of the THERMALIZATION spectral code. Subsequently, the data were collapsed into the 30 groups of the THERMOS library of the V.S.O.P. code system. For calculating the transport cross sections, the 'outscattering' approximation was used. The average cosines of the laboratory scattering angles used in this approximation were determined from the P_1-components of the corresponding group-to group transfer cross sections.

In the case of graphite, the 97 group transport cross sections had already been generated for 17 different temperatures in the past. Now, the transport cross sections for the remaining scatterers on the THERMOS library were calculated, i.e. for Be-9, Be in BeO, BeO, H-1 in H_2O, H-2 in D_2O, and O-16. The different temperatures and scattering models used for generating the group cross sections are given in Table I.

The main calculation route for determining the group data for the scatterers is shown in Fig.1 and is as follows:

1. A multigroup data set given in the 97-energy-group structure of the THERMALIZATION spectral code (10^{-5} eV –

5 eV) is produced in the AMPX master library format [4] using the basic data from the ENDF/B-V, -VI, -VII or the JEF-1 library. In the case where thermal scattering data in the form of S(α,β) data are given on the ENDF/B-VI or VII tape, the master library is generated by the code NJOY [5] and the AMPX77 module SMILER. In the case where no explicit thermal scattering data are given on the ENDF/B-VI or VII tape the master library is generated by the XLACS module of the AMPX77 code system calculating the thermal scattering matrices with the free gas model.

2. Subsequently, the calculation of the transport cross sections is made by the 1-d transport code XSDRNPM of the AMPX77 code system using the P_1-S4 approximation and two kinds of cell calculations:
   a) in the case of H-1 in H_2O, H-2 in D_2O, and O-16 an eigenvalue calculation is made for a spherical homogenized unit cell with a radius of r = 3.54 cm, assuming a PBMR-pebble with 8 % enriched U and 9 g U/ pebble, 10 % water or heavy water in the space between the pebbles, and a white boundary condition at the outer surface of the cell.
   b) in the case of Be-9, Be in BeO, O in BeO, and BeO a fixed source calculation was made in a Be or BeO pebble with r = 5 cm assuming a volume neutron source and using thermal upscatter scaling and a white boundary condition at the outer cell surface.

In the unit cell calculations, no further condensation of the 97 group data was performed. The transport code XSDRNPM provides two options for generating transport cross sections which are based on the 'consistent' and 'inconsistent' method. These methods are also referred to as the 'outscatter' and 'inscatter' approximations because of the nature of the equations used. Since the neutron currents, which are required for the 'consistent' method, are not yet available at this stage of the calculation, the 'outscatter' approximation was chosen. The 97 group transport cross sections were punched by the AMPX77 module PAL and stored on theTHERMALIZATION library.

TABLE I
Scatterers on the THERMALIZATION and THERMOS-Library with New Transport Cross Sections Data

Scatterer	Temperatures of the Scatterer [K]	Thermal Scattering Model (Data Base)
Be-9	980	Crystal Model (ENDF/B-VII)
Be-9	1366, 1422	Free Gas Kernel (JEF-1)
Be in BeO	900	Crystal Model (ENDF/B-VII)
BeO	900	Crystal Model (ENDF/B-VII)
H-1 in H_2O	293.6, 323.6, 373.6, 473.6, 573.6	Bound Hydrogen (ENDF/B-VI)
H-2 in D_2O	323.6, 373.6, 473.6, 573.6	Bound Deuterium (ENDF/B-VI)
O-16	293.6, 323.6, 373.6, 473.6, 573.6, 900, 1200, 1350	Free Gas Kernel (JEF-1)

The way in which the individual scatterers were treated is illustrated in Fig. 1 and given in the following:

- Be-9: On the thermal ENDF/B-VII file, S(α,β) data are given for 8 different temperatures up to 1200 K. Therefore, the group averaged cross sections for the desired temperature of 980 K could be generated from the thermal basic data of the ENDF/B-VII file. They were calculated by the NJOY code using the crystal model at the temperatures T = 800 K and T = 1000 K, converted to the AMPX master interface by the SMILER module and interpolated by the AMPX77 module ICE in order to get the thermal data at T = 980 K. For the remaining two temperatures of

1366 K and 1422 K the thermal scattering matrices were calculated using the free gas model – similar to the thermal scattering model used for this material in the old THERMOS library. In this case, the Be-9 data were generated by the XLACS77 module of the AMPX77 code system using the JEF-1 basic data file.

- Be in BeO: The basis of the data for Be in BeO was the ENDF/B-VII file, where S(α,β) data are given for 8 temperatures from 296 K up to 1200 K. Using these ENDF/B-VII basic data multigroup cross sections were calculated by the NJOY code for the two temperatures T = 800 K and 1000 K and converted by the SMILER module into the AMPX master library format. In order to obtain the data at the required temperature of 900 K an interpolation between the data for T = 800 K and T = 1000 K was made using the AMPX77 module ICE.
- BeO: In order to calculate the group cross sections for BeO, the group data of O in BeO – the basic thermal scattering data are given in the form of S(α,β) data on the ENDF/B-VII file similar to the basic data of Be in BeO – were calculated by the NJOY code, converted to the AMPX master library interface and interpolated in order to get the thermal data at T = 900 K. The resulting data were added to the group data of Be in BeO by the use of the AMPX77 module ICE. The transport cross sections were generated by the XSDRNPM module as described under point 2b.
- H-1 in H_2O and H-2 in D_2O: The basic thermal scattering data of H-1 in H_2O and H-2 in D_2O are given as S(α,β) data at 8 different temperatures from 296 K up to 1000 K on the ENDF/B-VI tape. The group averaged data sets on the AMPX master tape were generated by the NJOY code and the AMPX77 module SMILER. The transport cross sections were generated as described above.
- O-16 in H_2O and in D_2O: The scattering by the oxygen atom in the water or heavy water molecule is not included in the tabulated scattering law data for water or heavy water on the ENDF/B-VI or VII files. It was taken into account by adding the free gas scattering data oxygen of mass 16. Thus, the thermal scattering matrices of O-16 were calculated by the AMPX77 module XLACS using the free gas model and the transport cross sections were generated in a calculation similar to the unit cell calculation used for H-1 and H-2.

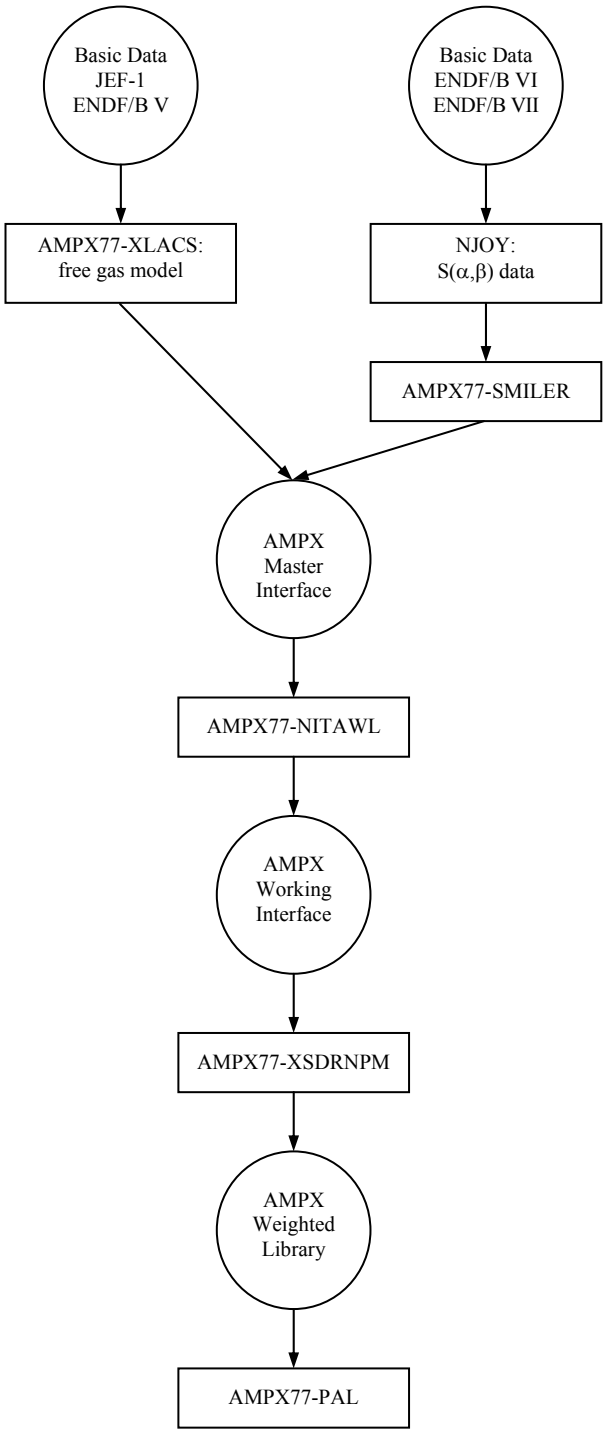

Fig. 1 Procedure for producing the group cross sections.

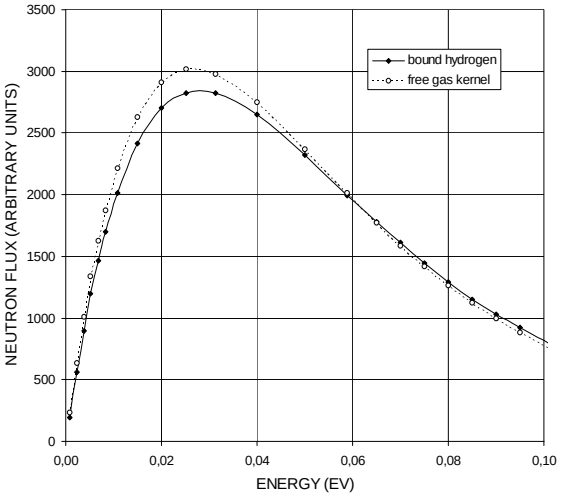

Fig. 2 Neutron spectra in water at T = 300 K with Σ_{abs}/N_H = 2.67 barn.

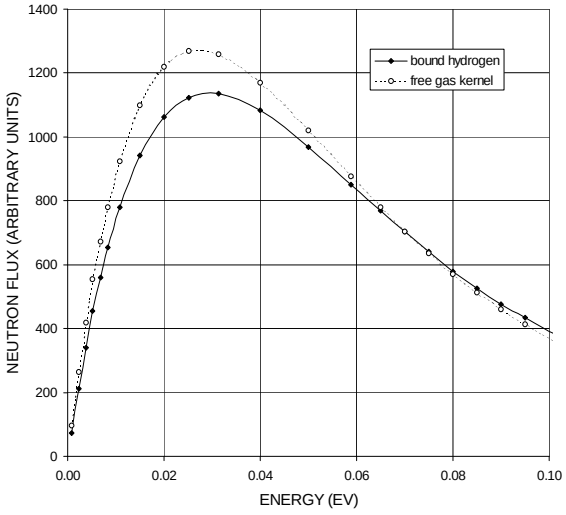

Fig. 3 Neutron spectra in water at T = 300 K with Σ_{abs}/N_H = 5.4 barn.

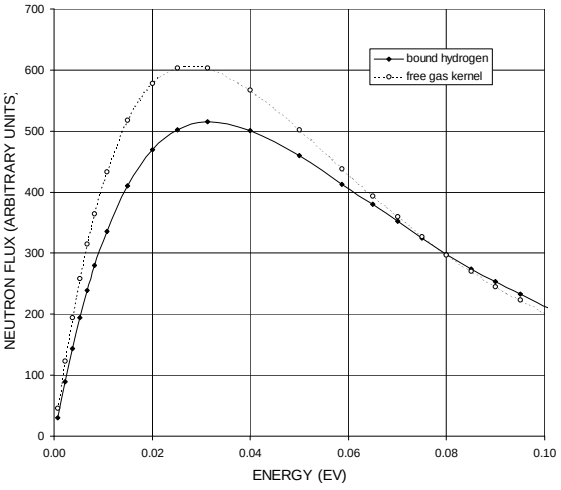

Fig. 4 Neutron spectra in water at T = 300 K with Σ_{abs}/N_H = 9.6 barn.

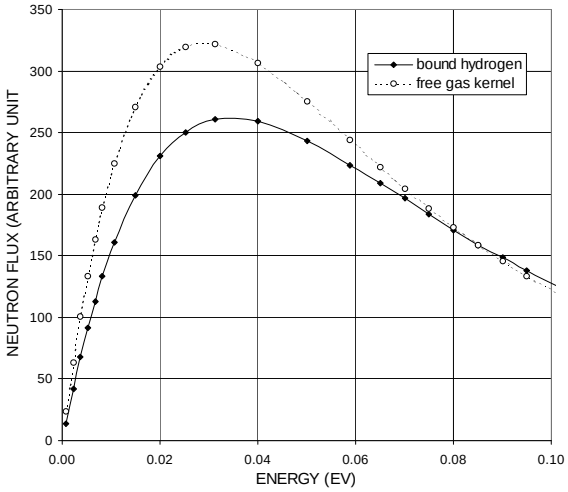

Fig. 5 Neutron spectra in water at T = 300 K with Σ_{abs}/N_H = 15.4 barn.

Update and Test of the New Scattering Matrices

After finishing the update procedure for the thermal transport cross sections it was started to update the scattering matrices on the thermal library of the V.S.OP. code system as well by converting the data given in the AMPX master library format into the THERMALIZATION format. Before the corresponding data are finally incorporated into the library some test calculations with the new data were made. For this purpose and in order to show the influence of the scattering model on the thermal neutron spectrum, a comparison between the bound-atom model and the free gas model was accomplished for water. Similar test calculations had also been made for graphite in the past.

The thermal neutron energy spectrum was calculated in a water sphere poisoned with cadmium sulfate in four different concentrations using scattering cross sections of water determined from the bound-atom model and the free gas model. In the poisoned water sphere of r = 5 cm thermal neutron spectra were calculated by the transport code XSDRNPM for a water temperature of T = 300 K using the S_4-P_1 approximation. A fixed volume neutron source was used and a white boundary condition at the outer surface of the cell. The group constants of water given in a 97-energy-group structure in the thermal energy range from 10^{-5} eV up to 5 eV were based on the ENDF/B-VI file and generated by the NJOY code in the case of the bound-atom model and by the XLACS77 module of the

AMPX77 code system in the case of the free gas model.

The water was poisoned with cadmium sulfate in four different concentrations so that the microscopic absorption cross section for a neutron of 0.025 eV energy was 15.4, 9.6, 5.4, and 2.67 barn. The different extents of cadmium poisoning were chosen in order to increase the sensibility of the spectrum to binding effects. For much less cadmium the spectrum would be close to a Maxwellian no matter what the mechanism of thermalization is, whereas for much more cadmium, relatively few neutrons would reach thermal energies.

It can be seen from the Figs. 2 through 5 shown below that the effects of atomic binding in light water are substantial at the highest cadmium poisoning. In all calculations, in which the chemical binding of the H-atom in H_2O is considered, the thermalization of the neutron is not as good as in the case of the free gas model. The consequence is that the maxima of these neutron spectra will be lower because not so many neutrons will reach the thermal energy range.

The neutron spectra decrease with increasing $CdSO_4$ concentration in the water as can be seen in the Fig. 2 through 5 because more neutrons will be absorbed, but the relative percentage deviation between the maxima of the corresponding deviation between the maxima of the corresponding neutron spectra – calculated on the one side with the bound hydrogen model and on the other side with the free gas model – becomes greater: from 6.3 % at the lowest concentration of cadmium sulfate with Σ_{abs}/N_H = 2.67 barn up to 19 % at the highest concentration with Σ_{abs}/N_H = 15.4 barn.

Summary

At present the process for updating the thermal cross sections used in the V.S.O.P. code system has reached the following status. The group averaged cross sections and the scattering matrices for graphite, hydrogen in H_2O, deuterium in D_2O, Be-9, Be in BeO, and BeO were recalculated on the basis of the latest ENDF/B-VI and ENDF/B-VII data for all temperatures required by the V.S.O.P. code. On the basis of these data new 97 group thermal transport cross section were calculated and collapsed to the 30 group structure of the THERMOS library of the V.S.O.P. code system. It was begun to update also the remaining thermal cross sections used in the V.S.O.P. code by converting the new cross section data given in the AMPX master library format into the format of the THERMALIZATION library. Furthermore, test calculations with the new cross section data were made in which the effect of the scattering matrices calculated for bound-atom systems was compared with that of the scattering matrices obtained by the free gas model.

References

[1] P.F. Rose and C.L. Dunford, “ENDF-102, Data Formats and Procedures for the Evaluated Nuclear Data File ENDF-6”, BNL-NCS-44945, Brookhaven National Laboratory (1991).

[2] H.C. Honeck, “THERMOS: A Thermalization Transport Code for Reactor Lattice Calculations”, BNL 5826, Brookhaven National Laboratory (1961).

[3] H. J. Rütten, K. A. Haas, H. Brockmann and W. Scherer, V.S.O.P.(99/05) Computer Code System, Jül-4189, Forschungszentrum Jülich (2005).

[4] N.M. Greene et al., “AMPX-77: A Modular Code System for Generating Coupled Multigroup Neutron-Gamma Cross-Section Libraries from ENDF/B-IV and/or ENDF/B-V”, ORNL/CSD/TM-283, Oak Ridge National Laboratory (1992).

[5] R.E. MacFarlane, “The NJOY Nuclear Data Processing System, Version 91”, LA-12740-M, Los Alamos National Laboratory (1994).

Operational behaviour of catalytic recombiners – experimental results and modelling approaches

E.-A. Reinecke[1], S. Struth[1], S. Kelm[1], Ch. Granzow[1], T. Zgavc[1], U. Schwarz[2]

[1] Institute for Energy Research / Safety Research and Reactor Technology (IEF-6), Forschungszentrum Jülich GmbH /
[2]Institute for Reactor Safety and Reactor Technology, RWTH University of Aachen
Corresponding author : e.reinecke@fz-juelich.de

Passive autocatalytic recombiners (PAR) are implemented in LWR containments as an accident management measure to mitigate the consequences of a possible hydrogen combustion in the course of a severe accident. The performance of a PAR has been demonstrated in large scale tests; however these integral tests provided no data for detailed model development. At Forschungszentrum Jülich separate effect tests are performed in order to obtain experimental data suited for the validation of detailed numerical models for the assessment of the operational behaviour of PAR.

Two modelling strategies are pursued. The detailed evaluation of the reaction kinetics and heat and mass transport phenomena on a single catalyst element is performed by a direct implementation of the transport and kinetic approaches in the commercial CFD software ANSYS CFX 11. To model the interaction of PAR with the containment and address the issues mentioned above, REKO-DIREKT, a detailed user model based on Fortran 90 will be implemented in CFX to model the entire PAR. This in-house code is already validated against the database and capable to model all relevant processes.

Introduction

During severe accidents (SA) in light water reactors, hydrogen is produced by the exothermal oxidation of the fuel claddings, hot metallic components and after failure of the reactor pressure vessel and melt relocation to the reactor pit due to decomposition of concrete as well. These processes produce hydrogen with such high rates and for a long term in the course of a SA that the local volumetric concentrations inside the containment exceed the lower flammability limit. Both major nuclear accidents of Three Mile Island (TMI) in 1979 and Chernobyl in 1986 resulted in a world-wide investigation of SA and the hydrogen risk.

Passive autocatalytic recombiners (PAR) are implemented in LWR containments as an accident management measure to mitigate the consequences of a possible hydrogen combustion. In the frame of SA analysis reliable numerical models are a vital element for the assessment of PAR performance and efficiency. International research activities e.g. in the European FP-6 Network of Excellence SARNET (Severe Accident Research NETwork) investigate related aspects. The important modelling issues are on the one hand the phenomena inside the PAR, e.g. the buoyancy driven flow and hydrogen depletion due to the catalytic surface reaction. On the other hand, its interaction with the containment atmosphere in particular the PAR outflow and its influence on the mixing process, the inducing of natural convection by the hot PAR box housing, and the effect of forced flow conditions are addressed. Safety related criteria such as possible gas-phase ignitions caused by hot parts due to the exothermal reaction are considered as well.

Experimental studies

Numerous integral experiments have been performed in the past aiming at demonstrating the PAR performance under realistic conditions. However, developing detailed numerical models from these integral and mostly transient data represents a difficult if not impossible task leading to “black-box” models which have a limited application range and do not cover all relevant parameters to sufficiently deal with the above-mentioned issues. In order to fill existing gaps in knowledge and complement the scientific data base, detailed experiments are performed at the Institute for Safety Research and Reactor Technology (IEF-6) at Jülich. In the small-scale test facility REKO-3, representing a recombiner section, detailed investigation of the reaction kinetics under well-defined and steady-state conditions has been performed. Currently a new large test vessel REKO-4 is under construction for testing PAR behaviour under natural convection conditions. It will provide various possibilities for instrumentation to measure temperatures and gas compositions and in particular it will be equipped with particle image velocimetry (PIV) for measuring the flow field around the PAR.

The REKO-3 test facility (Fig. 1)allows the investigation of catalyst samples inside a vertical flow channel under well defined conditions comprising gas mixture, flow rate and inlet temperature. The catalyst sheets (stainless steel coated with washcoat/platinum catalyst material) are arranged in parallel forming vertical rectangular flow channels. Such a set-up represents a box-type recombiner section of AREVA design. Inside of the configuration the distribution of the catalyst temperatures and the gas com-

position in vertical flow direction are measured. The correlation of the hydrogen conversion and catalyst temperatures with the experimental parameters serve basically to clarify the interactions of reaction kinetics, heat and mass transfer, and the flow conditions inside the recombiner.

(a)

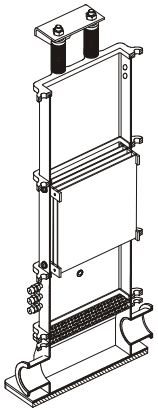

(b)

Fig. 1: REKO-3 test facility
(a) partially isolated, (b) schematic view

Typical measurement results are given in Fig. 2. These steady-state distributions of the hydrogen concentration (left side) and the catalyst temperature (right side) were obtained at 2 vol.% and 4 vol.% inlet hydrogen concentration, the inlet gas temperature of 25°C and a flow rate of 0.8 m/s. The symbols represent measuring values with lines added for the sake of clarity. The measured values are plotted on the horizontal axis in order to illustrate the vertical arrangement of the catalyst plates.

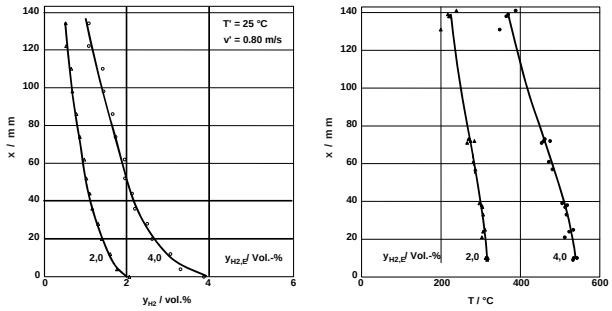

Fig. 2: Steady-state hydrogen depletion (left side) and catalyst temperatures (right side) along the catalyst sheets for two different hydrogen inlet concentrations at 25°C inlet temperature and a flow rate of 0.8 m/s

Specific attention has been paid to the effect of steam and oxygen starvation on the conversion rate as described by Drinovac (2006). On-going experiments deal with the ignition of the gas mixture on hot catalyst sheets (Tab. I).

Table I. Experimental results and model validation matrix

issue	*experiments performed*	*validation performed*
standard reaction kinetics	x	x
influence of steam	x	x
lack of oxygen	x	x
surface ignition	on-going	

In order to study the operational behaviour of PAR under natural flow conditions and to study the chimney effect on the PAR operation in detail a new facility (REKO-4) is presently constructed at Jülich. The pressure vessel with an inner diameter of 1.4 m and a height of 4 m is designed for a pressure of 25 bar (Fig. 3).

A total of 25 flanges will allow the accessibility of the vessel with different measurement techniques. Foreseen measurements inside the vessel are basically pressure, gas temperature and hydrogen/oxygen concentration. The PAR device will be equipped with thermocouples for catalyst and gas temperature measurement and hydrogen/oxygen sensors. Most challenging measurement will be the use of particle image velocimetry (PIV) for the measurement of the flow field at the inlet and the outlet of the PAR. These data are essential in order to determine the PAR throughput and efficiency. Furthermore, this high-resolution measurement technique provides data suited for CFD validation.

In the experiments aspects of the operational behaviour of small PAR devices will be studied when the flow rate is solely induced by the heated catalyst sheets. For this purpose, a defined amount of hydrogen will be released into the air-filled vessel. With the option of positioning the PIV device in different locations it is expected to visualise the flow pattern in different relevant areas around the PAR. First experimental results are expected for late 2008.

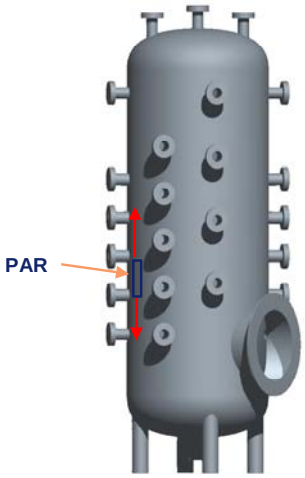

Fig. 3: REKO-4 vessel (schematic view)

Modelling approaches

There are several effects and phenomena related to PAR which need to be resolved in a higher detail than presently possible with lumped parameter (LP) codes and black-box models. These include local containment studies concerning the interaction of different safety measures as well as the detailed investigation of the thermo hydraulic phenomena inside a PAR. For these purposes different approaches have be developed at Jülich in order to model the catalytic surface reaction as well as the entire device. The simplest approach is the direct implementation of the manufacturer's empirical parameter correlations for calculating the hydrogen consumption rate. A more detailed approach is the implementation of REKO-DIREKT, a mechanistic model to describe an entire PAR via USER-Fortran routines. For a detailed understanding and optimisation of the thermo hydraulic and transport phenomena CFD is used to model the reaction and all relevant transport phenomena at a single catalyst element.

The REKO-3 test series revealed that in the present case the rate determining step of the catalytic recombination of hydrogen and oxygen is the transport of the products and educts from and to the surface. The implemented CFD model is based on this elementary understanding. For the simulation of the catalytic process only the transport of the species is considered. The outer surface of the catalytic coating is modelled as a wall. The chemical reaction is implemented as a single step reaction

$$H_2 + \tfrac{1}{2} O_2 \rightarrow H_2O + \Delta h_r^o$$

by means of sinks and sources of mass, enthalpy and momentum in the cells adjacent to the wall.

The prediction of the reaction rate is done by fully resolving the species boundary layer, which allows solving the reactants flux by Fickian diffusion only. So that the reaction rate can be described as

$$\dot{r}_i'' = \bar{c} \cdot \left(D_i + \cancel{\frac{\nu_t}{Sc_t}}^{\sim 0} \right) \frac{\partial X_i}{\partial y}\bigg|_w \qquad i : H_2, O_2$$

where c is the molar concentration of the mixture, D_i is the effective diffusion coefficient of the species i in the mixture, ν_t/Sc_t is the turbulent diffusion coefficient and X_i the molar fraction of the species i. To enable the model to predict also the reaction rates under oxygen starvation conditions the transport of oxygen is also considered. The system of compressible Navier Stokes equations is closed by the k-w based shear stress transport (SST) turbulence model in order to use this low Reynolds approach and integrate up to the wall and avoid the use of wall functions. The i-species are described by the ideal gas equation of state. As buoyancy is the major driving force, the full buoyancy model including the production and dissipation of turbulence is included. The radiative heat transfer between the plates and also with the environment is considered by a Monte Carlo model.

This modelling approach has been developed under application of the ERCOFTAC best practise guidelines (Casey and Wintergerste, 2000) and validated against the REKO-3 test series for plate type catalyst sheets (AREVA design). Figure 4 shows exemplarily the temperature profiles in the catalyst sheets and the hydrogen concentration decay in the flow channel for different hydrogen inlet concentrations and a typical flow velocity of 0.8 m/s in a PAR.

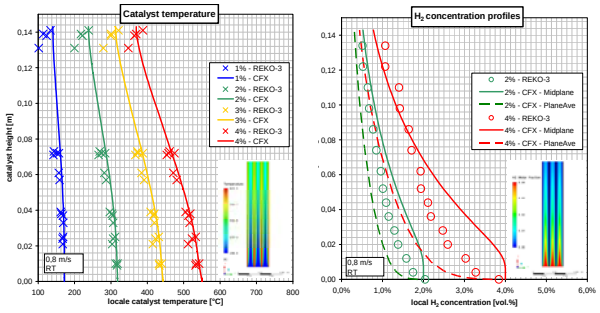

Fig. 4: Temperature und concentration profiles: Experimental and CFD modelling results

The catalyst temperature profiles are predicted quite well by the model, except a slight over prediction at the end of the catalyst sheet in some cases due to some uncertainties with regard to the radiative heat exchange with the REKO-3 channel and outlet. Comparing the concentration profiles with the experimental data is difficult as this measurement allows no point or profile measurement, so for validation purpose two extreme cases are considered: The values at the symmetry plane between the plates (solid line) as a quasi point measurement and an arithmetic average over the channel cross section (dashed line). The numerical model predicts the concentration profiles, and with it the entire reaction rate quite well in a reasonable agreement to the experimental results.

This modelling approach has its advantage in predicting the detailed thermo hydraulic and transport phenomena in a PAR channel and is used for the assessment of new catalyst designs. For the study of an entire PAR operational behaviour it is to cost intensive to model all catalyst elements this degree of detail.

Up to now for the PAR system design and accident analysis the only available and for designated cases validated models are the manufacturer's correlations which are implemented in integral LP containment codes. These empirical correlations are based on the large scale experiments performed to demonstrate PAR performance under realistic conditions (Bachellerie et al. 2003). These empirical models are validated for the specific experi-

mental conditions present in the original tests. However, for detailed CFD studies they do not provide relevant parameters, such as catalyst or box temperature to assess the ignition risk. For this reason, REKO-DIREKT, a 2D detailed mechanistic black-box model based on Fortran 90 was developed at Jülich (Böhm, 2006). For a single channel local reaction rates are calculated by means of a mechanistic transport approach

$$\dot{r}_i'' = Sh \cdot \frac{D_i}{d} \cdot \Delta C_i \qquad i : H_2, O_2$$

Here *Sh* is the local Sherwood number, D_i the effective diffusion coefficient of the species i in the mixture, *d* the hydraulic diameter and ΔC_i the molar concentration of the species i. The system of mass and energy balances is solved directly, which allows gaining a fast and robust solution. This single channel is extrapolated to a full recombiner catalyst section to calculate in a last step the buoyancy driven flow through the PAR box as well as the radiative and convective heat fluxes from the PAR to its environment. REKO-DIREKT provides also the efficiency of the PAR and the maximum catalyst temperatures which can be used for further risk and safety assessment. The code has been validated against the REKO-3 database.

Natural convection trough the PAR box is already implemented and predicts credible values for the flow velocity, compared to the integral large scale experiments. As these experimental database of the integral experiments are mainly not accessible and detailed enough, this phenomenon will be investigated in more detail at the REKO-4 test vessel, and give a more quantitative validation data base.

In the frame of SARNET, PAR interaction studies (PARIS) are performed in order to investigate adopted models and approaches and focus on the impact of PAR elevation on the phenomena of stratification (PARIS-1). In the frame of this study an AREVA FR90/1-150 like PAR was considered in a 2D rectangular domain. The hydrogen conversion was modelled by means of the empirical AREVA correlation. In PARIS-1 a closed 5mx5m domain, fitted with two PARs was addressed (Fig. 5). The starting point for the 3000 seconds calculation was a homogeneous mixture at 100°C, containing 5 vol.% H_2 in dry air and steam at saturation conditions. In the first 300 seconds the flow was nearly symmetric (Fig. 5, left) and resulted after about 400 seconds in a stable thermal stratification in the domain. As thermally driven convection loops have difficulties to mobilise the cold H2 rich gas located near the floor below the PAR inlet (Fig. 5, right), this scenario develops into a diffusion controlled situation. The elevation of the PARs had an influence on the thickness of the bottom layer, but could not resolve it anyway.

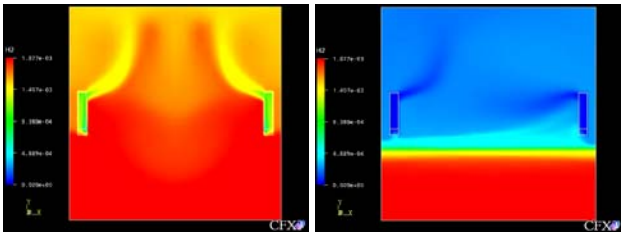

Fig. 5: PARIS-1: Hydrogen mass fractions operation after 10 s and diffusion controlled scenario after 400 s

The main reason for the formation of the bottom layer was the artificial assumption of adiabatic walls. In a real situation heat transfer to the compartment walls and condensation would result in an enhanced mixing of the atmosphere. This was demonstrated in a further calculation with constant wall temperatures revealing that the bottom layer is dissolved after 500 s. Nearly adiabatic situations are however imaginable and the phenomenon of thermal stratification has occurred in some integral containment experiments. Consequently, the relevance of detailed studies has been affirmed by this benchmark exercise.

Outlook

Based on these experimental results a detailed model has been developed and implemented in CFX for describing the H2 conversion process at a single catalyst element. This model will be used for the optimisation and design of innovative catalyst designs. In order to model an entire PAR currently the manufacturer's correlations are directly implemented in CFX. To overcome the limitations of these empirical parameter models, REKO-DIREKT, a mechanistic model will be implemented by means of USER Fortran routines. First common recombiner interaction studies within SARNET affirm the need of detailed investigation of PAR operational behaviour. This work will be continued in the SARNET and at Jülich.

References

E. Bachellerie, et al., State-of-the-art Report on Passive Autocatalytic Recombiners - Handbook Guide for Implementing Catalytic Recombiners, Technicatome Company Report, Technical Note TA-185706 Ind. A. (2002).

J. Boehm, Modelling of the processes in catalytic recombiners, Forschungszentrum Juelich, Series Energy Technology, Volume 61 (2007).

P. Drinovac, Experimental studies on catalytic hydrogen recombiners for light water reactors, PhD, on-line publication, RWTH Aachen (2006).

E.-A. Reinecke et al, "Studies on innovative hydrogen recombiners as safety devices in the containment of light water reactors", Nuclear Engineering and Design 230 (2004) 49-59

A SOPHISTICATED MONTE-CARLO-CODE SYSTEM FOR CORE PHYSICS AND SAFETY ANALYSIS USING HIGH-PERFORMANCE COMPUTERS

R. NABBI
Institute of Energy Research - Safety Research and Reactor Technology IEF-6
Leo-Brandt-Straße, 52425 Jülich, Research Centre Jülich, Germany
E-Mail: r.nabbi@fz-juelich.de

ABSTRACT

For the simulation of complex core physics processes and fuel depletion, a sophisticated computer code system was developed on the basis of the Monte-Carlo-Method (MCNP) and a burnup code (BURN) for running on parallel high-performance computers. The whole model of the coupled code system (MCN-BURN), applied to the high power research reactor FRJ-2, consists of a detailed nodalization of the reactor core and surroundings with 11250 material cells of different geometry and varying isotopic composition. The accuracy of the model was verified by the simulation of criticality experiments and comparison with the measured distribution of average and local neutron flux density. The verification was extended to a long period of power history including recent measurements. The reactivity value of each individual core configuration at any burnup step could be predicted within 2σ standard deviation. The local neutron flux was determined with a deviation of less than 5 %. The whole core physics model of MCNP-BURN was applied to determine the distribution of fission power in the individual fuel elements of the whole core as well as the safety parameters for different HEU and LEU core configurations and fuel composition.

1. BACKGROUND

In view of the limitations of the standard deterministic methods in geometrical and numerical modeling, Monte-Carlo methods offer the potential for high-precision analysis /1/. Based on the rapid progress in computer technology and development of numerical methods and resulting High-Performance computing, the Monte-Carlo methods proved to be as indispensible tools for handling complex neutron transport problems and large nuclear datasets. In parallel with this development and need for a sophisticated code system the Monte-Carlo code, MCNP was employed for the analysis of core physics, safety characteristics of common reactor systems /2/. The code is coupled with a comprehensive pointwise contineous-energy cross section data library allowing detailed simulation of nuclear processes and is capable of modeling any complex fuel element geometry and core configuration /3/.

Due to the steady state character of the models of MCNP it was necessary to make a coupling with a depletion code (BURN) to simulate the variation of the material composition taking place during the fuel burnup and power history, respectively /4,5/. The code package (MCNP-BURN) was employed for the core physics analysis of the German high power research reactor FRJ-2 and approved by the German licensing authority after the verification campaign based on neutronic measurements and criticality experiments. The verification process was extended to the long term range by the simulation of different operating cycles with various core loadings and configurations/6/. The present paper describes the development and capability of the MCNP-BURN code and the results of the comprehensive simulation of the core physics for the case of FRJ-2.

2. CORE PHYSICS SIMULATION OF FRJ-2

The FRJ-2 is a heavy water moderated tank-type research reactor consisting of 25 so-called tubular MTR fuel elements (FE) arranged in five rows of fuel elements (Fig. 1). The tank is surrounded by a graphite reflector 0.6 m in thickness enclosed within a double-walled steel tank. The active part of the tubular fuel elements is formed by four concentric tubes having a wall thickness of 1.5 mm and a length of 0.63 m. The tubes consist of fuel meat clad with pure aluminum and are accommodated in a shroud tube 103 mm in diameter. The fuel meat contains UAl_x in an aluminum matrix with a U235 enrichment of 80 %. The annular water gap between the tubes has a width of about 3 mm leaving a central hole of 50 mm diameter filled with a thimble for irradiation purposes.

The reactor is equipped with two independent and diverse shutdown systems, the coarse control arms (CCAs) and the rapid shutdown rods (RSRs). The CCAs are lowered and raised manually around a pivot in order to control power levels during normal operation, whereas the RSRs are permanently in their upper position.

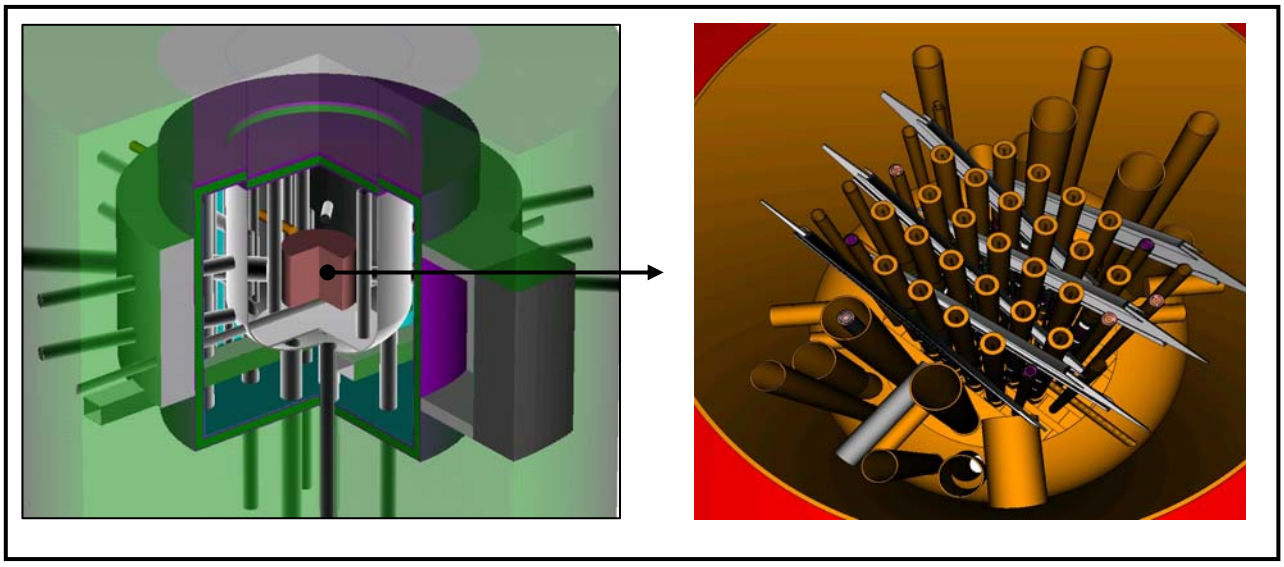

Fig. 1: MCNP model of the reactor (left) and core (right) with the arrangement of the fuel elements and shutdown system (for simulation on High-Performance Computers)

3. MCNP MODEL AND BURNUP RECYCLING

The MCNP model of FRJ-2 is a complete 3-dimensional full-scale model with a very high level of geometric fidelity. It comprises the reactor core, CCAs, core structures, beam tubes, the graphite reflector and the biological shield. The core region consisting of 25 fuel elements was modeled as a cylinder containing a square lattice with an array of cells representing the individual fuel elements. Each cell in the lattice contains a detailed model of each fuel element comprising the internal thimble, 4 circular fuel tubes and the borated outer shroud tube. Each individual cell is divided into 15 axial and 35 radial and azimuthal material zones. The detailed segmentation of the whole core resulted in a model with 11 250 material cells. The MCNP model of the core and

Due to the continuous change of the material composition in the fuel meat resulting from fuel consumption, every fuel segment of the MCNP model is coupled with a fuel depletion model (BURN). In this way the variation of the neutronic states of the core is simulated by multiple linked burnup and MCNP calculations. In each time step - representing a time interval in the operation history - fuel burnup is determined on the basis of neutron cross sections and local flux from the previous step of the MCNP run. The resulting local nuclide densities –zone-wise- are used in the next step of calculations with MCNP to generate the flux distribution and one-group cross-section data for the next burnup step. As an example of the MCNP-BURN run the flux shape in the core and in the individual fuel element at the core midplane is given in Fig. 2.

To achieve a sufficient number of neutron tracks and score in all cells and consequently to reduce the estimated error of the physical values (keff and local neutron flux) all simulations were run for 1000 cycles each with 1000 particle histories. By the statistical evaluation of 1 Mio. histories, a standard deviation of 0.001 was achieved for the multiplication factor (i.e. 0.10 % dk/k) and 0.05 for the local n-flux

.

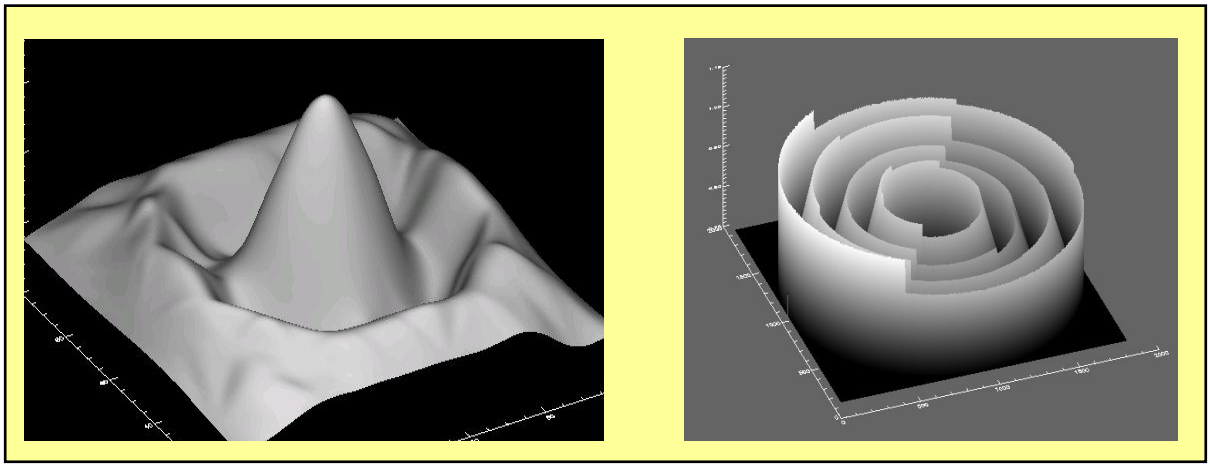

Fig. 2: Neutron flux distribution in the core (left) and in a fuel element (right) facing the core center line from the left side (MCNP-tallies)

5. RESULTS OF SIMULATIONS

5.1 Criticality States

The neutronic and criticality behavior of FRJ-2 was studied in detail by the simulation of past operating cycles with various core configurations and burnup distribution. In order to verify the geometrical model and the employed depletion routine, the criticality state (representing the multiplication factor) of the reactor core was considered for comparison. For this purpose the eigenvalue was calculated for different burnup states and angles of the CCAs and compared with the critical angle known from the critical experiments at the beginning of a cycle and during operation. Accordingly (Fig. 3), the criticality state of the core at each time and burnup step is reproduced with a maximum deviation les than 0.5 % dk/k representing the accuracy of the model in the simulation of the neutronic conditions of the core. Due to the accurate calculation, the model is used to predict the reactivity value of the core of the actual operating cycle for refueling the core and shuffling the fuel elements. The criticality after reloading the core is achieved as predicted by the model with a deviation of 0.4 % dk/k amounting to the 2σ confidence interval.

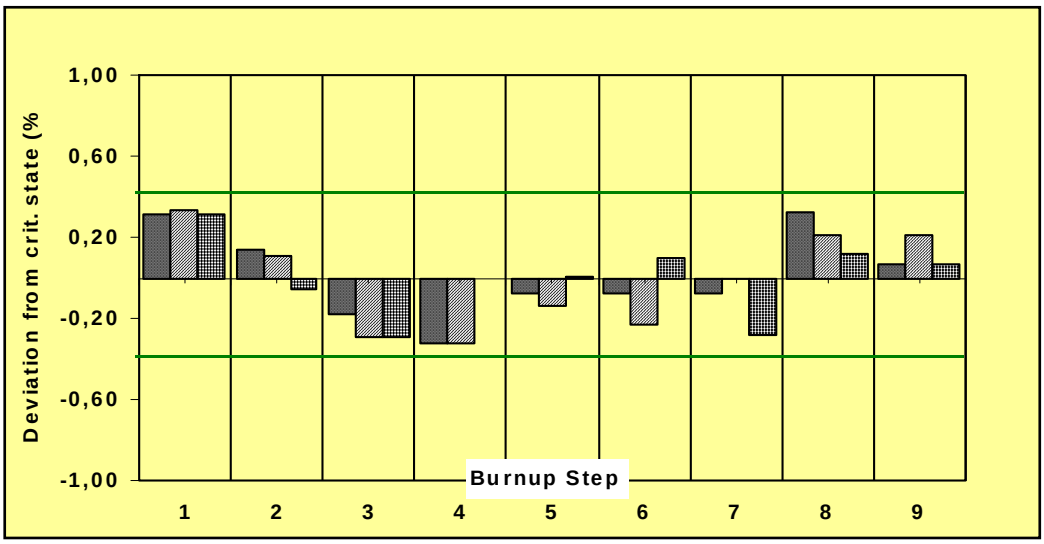

Fig. 3: Deviation of the calculated multiplication factor from the reference value as a function of burnup step for 3 operating cycles

5.2 Average and Local Distribution of n-Flux

The distribution of the average neutron flux in the core and in a fuel elements is given in Fig. 4. for comparison with the recent measurements performed during the 1st operating cycle in 2005. For these results, cobalt foils were irradiated in the central channels of all fuel elements. Taking the uncertainties of the measuring method resulting from the irradiation time and positioning of the foils into consideration, the calculated values are in good agreement with the experimental results in the whole core and after many cycles. The maximum flux appears in the central fuel element and decreases towards the outer positions.

In addition to the relative flux factors, the axial distribution of the n-flux was calculated in the central channel of the highest rated fuel element and compared with the results of the local measurement. The corresponding n-flux profile given in Fig. 4 was calculated from the reaction rate by using one group cross-section data. For this purpose the rate of the (n,γ) reaction for Co-59 was determined with MCNP-BURN. Due to high number of history, the simulation of the irradiation experiment resulted in an standard deviation of 4 %. According to Fig. 4 the maximum deviation between the measurement and calculation amounts to 5 %. The maximum n-flux in the inner channel of the highest fuel element amounts to 2.80E14 n/cm²s at 20 MW power level. A comparison of the measurements and calculations for different core configurations and loadings over a long period of power history shows that the coupled models of MCN-BURN is capable of precisely simulating the neutronic state of every core and verified for the calculation of flux, power and burnup distribution including safety parameters.

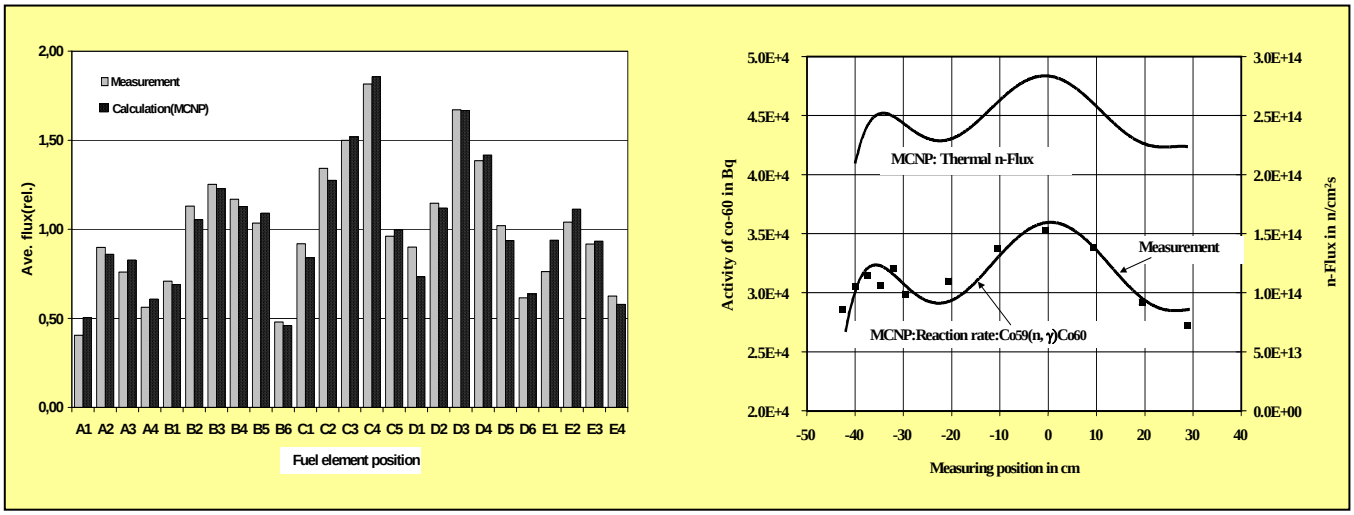

Fig. 4: Comparison of calculation by MCNP-BURN and measurement of the n-flux Distri-bution in the core (left) and in the central fuel element (right)

6. References

/1/ *E. Lewis & W. F. Miller Jr.*, Computational Methods of Neutron Transport, John Wiley & Son New York, 1984, 401 pp. (Republished by Am. Nucl. Soc. 1993)

/2/ *J. F. Briemeister Ed.* MCNP- A General Monte Carlo N-Particle Transport Code LA-12625-M, Version 4B, Los Alamos National Laboratory, March 1997

/3/ *F. Rahnema et al.*, Comparison of ENDF/BV and VI.3 for water reactor calculations Proc. Ann. Mtg. of American Nuclear Society, Vol. 76, pp. 324-325, June 1997

/4/ *R. Nabbi et al*, "Application of Coupled Monte-Carlo and Burn-Up Method using High Performance Computers", ANS Conf. on MC Methods, Chattanooga, USA, 2005

/5/ *R. Nabbi, J. Wolters*,"Coupling MCNP and a Depletion Code for Detailed Neutronic Analysis and Optimum Core Management at the German FRJ-2 Research Reactor" Intn. Meeting on: Math. Methods for Nucl. Application, Sept. 2001, Salt Lake, USA

/6/ *R. Nabbi, G Damm*," A sophisticated Monte-Carlo-code system for the safety and core physics analysis of FRJ-2", ENS 9th Intern. Topical Mtg. on Research Reactor Fuel Management, RRFM 2006, April 2006, Sofia, Bulgaria

Thorium fuel rod irradiation and a LWR benchmark setup for the verification of neutronic codes

R. Nabbi[1], D.F. da Cruz[2], W. von Lensa[1] , M. Verwerft[3]

[1]*Forschungszentrum, D-52425 Juelich, Germany, r.nabbi@fz-juelich.de*
[2]*NRG, P.O. Box 25, 1755 ZG Petten, The Netherlands*
[3]*SCK•CEN, Boeretang, 200, B-2400 Mol, Belgium*

INTRODUCTION

The objectives of the LWR-DEPUTY project (funded by the European Commission) is to study to what extent the existing NPPs can create markedly less nuclear waste by moving to inert matrix fuels, so-called "*inert matrix fuels*" (IMF) or to ThO_2 based fuel. To demonstrate the deployment and performance of this type of next generation fuel comprehensive studies have been undertaken and reported worldwide [1-3].

The similarity of properties of thorium fuel with UO2 makes it suitable for the introduction and irradiation in the existing LWRs. Preliminary numerical evaluation and deployment in the NPP in Obrigheim, Germany (KWO), showed a good indication for high transmutation-performance and core safety [4]. Currently post-irradiation examinations (PIE) and radiochemical measurements are running aiming at the generation of a data base and benchmark suite for the verification of different numerical codes and data validation for the $(Th/Pu)O_2$ fuel.

The present work shows the modelling aspect and the results of calculation of the irradiation experiment carried out for the KWO irradiation on the basis of the sophisticated method using MCNP and ORIGEN[5,6].

REACTOR CORE AND IRRADIATION SETUP

For the investigation of the irradiation behaviour of thoria based fuel a $(Th/Pu)O_2$ fuel rod was inserted in the core of the KWO reactor and irradiated for 4 years (4 cycles) up to a burnup of about 38 MWd/kg. The carrier MOX-fuel assembly was a 14x14 unit consisting of 180 fuel rods and 16 guide tubes having the same length. The active part of the fuel rod consisting of 17 Th/Pu pellets with an enrichment of 3 w/o Pu_{fiss} was 146.5 mm and had an outer diameter of 9.5 mm.

The operating core of KWO with 97 fuel assemblies was designed for a cycle length of 326 effective full power days (efpd). In total 65 irradiated fuel assemblies (FA) together with 32 fresh fuel assemblies were loaded to the core. The core average burnup was 15.2 MWd/kg HM.

MCNP MODEL OF MOX-FUEL ASSEMBLY

For the generation of the benchmark setup and neutronic analysis a 3D model of the whole fuel assembly with the test fuel rod was made for the MCNP code of version 5 (Fig. 1). The model of the fuel rods did not consider axial spacers and endcaps but encompasses fuel cladding, gap and surrounding moderator zones in detail. For the outside boundary of the FA as well as the single rod calculation reflected boundary was applied on all sides. The initial fuel composition of the MOX fuel is taken from the UO_2 pin cell calculations according to the core average burnup. For the depletion calculation (ORIGEN) the power history of the FA was taken from the irradiation report [1]. The reactor power in the last operating cycle was 88 % rated power (of 1048 MW) at a initial boron concentration of 1300 ppm.

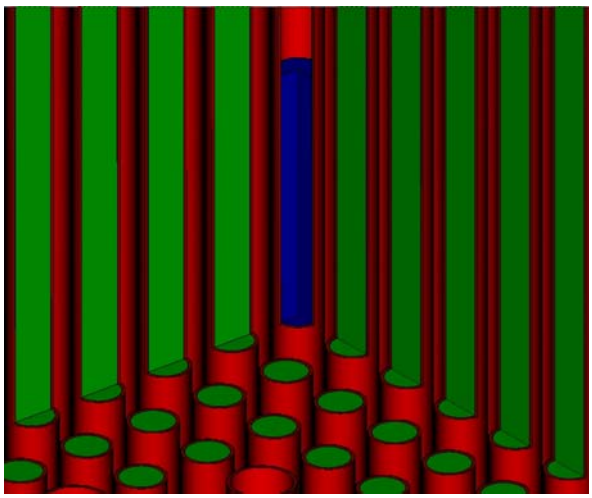

Fig. 1: MCNP model of the fuel assembly carrying the MOX fuel rods around the central rod ($Th/Pu\text{-}O_2$)

NEUTRONIC ANALYSIS

The variation of k-infinity over burnup is depicted in Fig. 2 together with the geometrical pin-cell and FA model. Accordingly it is slightly lower in the case of FA due to the effect of the surrounding fuel rods and moderator on the neutron spectrum.

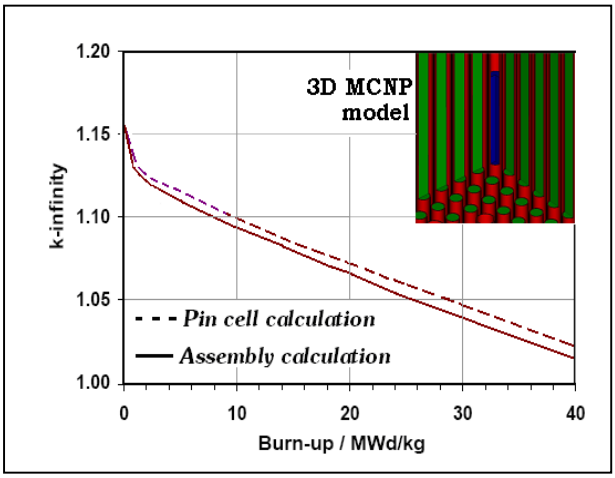

Fig. 2: k-infinity as a function of burn-up for the pin-cell and fuel assembly

The result of spectrum calculation is shown in Fig. 3 for the Th/Pu fuel rod as well as for a standard UO2 fuel rod of the same geometrical design (PWR) for comparison. Due to higher absorption cross section in the low energy range (resonance lines), the thoria based fuel exhibits a shifting of the spectrum from thermal to epithermal range. For the demonstration of this effect, the thermal part is additionally displayed in Fig. 3 in linear scale for both fuel types.

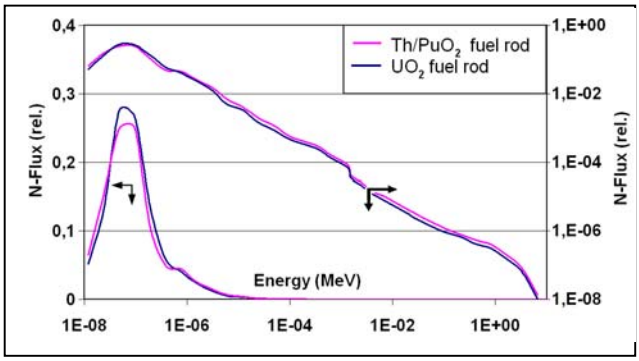

Fig. 3: Comparison of the neutron spectrum in the Th/Pu test and a standard UO_2 fuel rod (thermal range is separately displayed in linear scale for more detail)

The nuclear characteristics and spectrum are of significant effect on the distribution of burnup and therefore on the concentration profile of the fission products and actinides which are measured by radiochemical methods for comparison purposes. To study this effect the radial distribution the thermal flux within the whole assembly (Fig. 4) and in the test fuel rod was determined by a nodalized pin cell in the FA model . The results of the calculation are summarized in Fig. 5 for the test rod and in a surrounding MOX fuel rod as well as for a UO_2 fuel rod (as a reference).

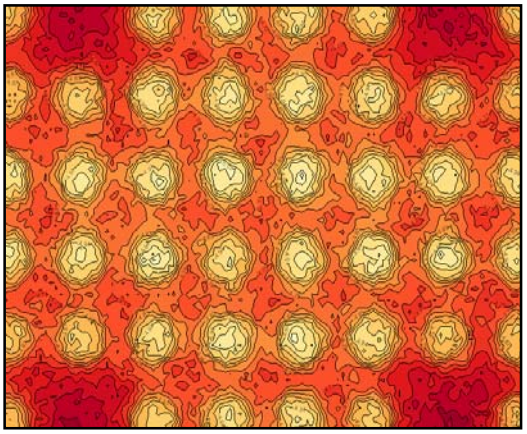

Fig. 4: Neutron flux pattern in the fuel assembly carrying MOX fuel rods and the test Th/Pu-O2 rod

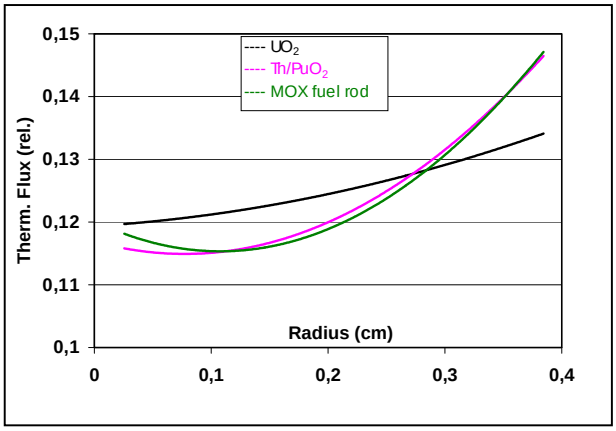

Fig. 5: Radial distribution of thermal flux in the fuel rod of different type

Accordingly the flux profile in the MOX and Test fuel rod is strongly varying (28 %) whereas the reference case (UO_2) shows a modest and flat distribution (14 %). This is caused by the relative higher absorption effect of Pu isotopes existing in the Th/Pu and MOX fuel rod, respectively.

Conclusions

The analysis shows that the neutron spectrum and spatial distribution in the thoria based fuel rod significantly differs from the uranium based fuel assembly. The local effects are of particular importance for the burnup behaviour of the irradiated fuel rod as the basis of the

experimental benchmark suite. The concentration of different isotopes (fission products and actinides) is strongly coupled with the radial shape of the flux and consequently needs to be measured accordingly. To reduce the numerical uncertainties the different codes involved in the project will be run on the basis of highly nodalized models.

REFERENCES

1. G. LOMBARDI, ET AL, "Neutronic analysis for U-free inert matrix and Thoria fuels for plutonium disposition in PWR", J. Nuclear Materials 274 (1999), p. 181-188
2. A. GALPERIN, ET AL, "Thorium Fuel for Light Water Reactors", Science & Global Security 6 (1997).
3. T. BODEWIG, "Optimized transmutation of Plutonium and Americium in PWR", Report of Research Centre Juelich, Juel-4131 (May 2004)
4. J. SOMERS, D. SOMMER,"Thorium Cycle: Development Steps for PWR and ADS Applications" EC-CONTRACT N°: FIKI-CT-2000-00042
5. J. F. BRIESTMEISTER (ED)," MCNP–A General Monte Carlo N-Particle Transport Code" LA-13709-M (2000)
6. R. NABBI, ET AL, "Application of Coupled Monte Carlo and Burn-Up Method using High Performance Computers" , ANS Conf. on MC Methods, Chattanooga, USA, 2005

SOPHISTICATED NEUTRONIC CALCULATION OF THE ITER UPPER PORT DIAGNOSTIC SYSTEM USING MONTE CARLO METHOD

P. BOURAUEL, R. NABBI
Institute of Energy Research - Safety Research and Reactor Technology IEF-6
Research Center Jülich
Leo-Brandt-Straße, 52428 Jülich - Germany
E-Mail: p.bourauel@fz-juelich.de

ABSTRACT

Research Center Jülich is involved in the development of a charge exchange recombination spectrometer (CXRS) for obtaining plasma parameters in the international fusion reactor ITER .For protection of the spectrometer from high temperatures and neutron flux, light from the plasma zone is guided through a mirror system and a glass fibre bundle. To perform nuclear analysis and to study the neutronic radiation load the Monte-Carlo-Code MCNP was employed. For this purpose a model with high fidelity of ITER and the Port Plug was used to acquire results of high accuracy. According to the results, the neutron flux at the first mirror is 7.3E+13 n/cm²s and decreases to 4.6E+7 n/cm²s at the back window. Due to continuous modification of the design a method was developed allowing flexible generation of the MCNP model and neutron transport simulation respectively.

1. Introduction

ITER (International Thermonuclear Experimental Reactor) is the international research and engineering proposal for an experimental project that will help to make the transition from today's studies of plasma physics to future electricity-producing fusion power plants. It will build on research done with today devices such as DIII-D, EAST, TFTR, JET, JT-60, TEXTOR, and will be considerably larger than any of them. The implementation of diagnostics on ITER will be a major challenge, as the environment will be much harsher. For example the levels of neutral particle flux, neutron flux and fluence will be respectively about 5, 10 and 10,000 times higher than in today's machines [1].

For the simulation of neutron transport in complex systems as the Port Plug structure of ITER different numerical methods are employed which are of deterministic or statistical character. Due to the complex geometry of ITER and the CXRS Port Plug encompassing inhomogeneous structures and components the MCNP Monte-Carlo-code has proven to be the solution for the study of the neutronic load on the components as well as for the calculation of the performance of the structures. The code is also extensively used worldwide in nuclear engineering to perform complex criticality studies and neutron and particle transport calculations [2].

Since the neutron flux distribution in the assembly is of importance to the operational performance of the components, lifetime, shielding performance and dose rate, detailed neutronic analysis and modeling are to be performed. In this work a sophisticated model was generated for the whole configuration of these components which was used for the determination of the flux distribution, nuclear heating and radiation damage.

2. Description of the CXRS Port Plug

ITER diagnostic equipment is integrated in six equatorial and 12 upper ports, five lower ports, and at many other locations in the vacuum vessel. The integration has to satisfy multiple requirements and constraints and at the same time must deliver the required performance.

The Charge Exchange Recombination Spectroscopy (CXRS) instrument analyses EM radiation in the visible region from the core and edge plasma regions in order to measure important parameters like temperature profile,

Helium ash density profile, Impurity density profile, plasma rotation, alpha particle confinement. The system will be installed at the upper port for measurements in the plasma core region. The CXRS system consists of the following subsystems: Collecting and re-imaging optics, fibre optic channels, spectrometers, detectors and data-acquisition.
Light emitted from the ITER plasma is collected by the front optics system. The light is guided through a labyrinth and imaged on the entrance surface of a bundle of fibre optic waveguides. Through the fibre optic waveguides the light is guided to a set of spectrometers of different types. The instrument will be installed in a port plug in diagnostic upper port #3. The upper port plugs are installed in the ITER Vacuum Vessel (VV) and includes a plasma-viewing first wall blanket shield module. Required mirror diameters are in the order of 35 cm which fits within the available cross-section of the port plug. However, design issues are seriously increased due to the following facts: The high amount of radiation in the front of the port plug precludes the use of transmissive elements, so that at the front opening only reflective optics can be used.
The first mirror is exposed to a high neutron and heat load and is in an environment where deposition of carbon is likely. Both leads to a high degradation rate of the first mirror and therefore protective measures are required to ensure the lifetime of the first mirror. Also the first mirror is exposed to large heat transients at the beginning of operation that may create a change in curvature of the mirror surface. The mirror material is one of the most important parameters to determine the rate of degradation. Presently the most likely option is to use a mirror made of mono-crystalline molybdenum. Furthermore, the mirror shall be placed in a retractable tube in order to be replaced after a while and a shutter will enable protection when CXRS is not functional between the shots. The shutter and the exchange construction are both mechanical moving systems. They should be simple in order to guarantee functionality. Fig. 1 shows the position of the CXRS port plug inside the ITER rector and the principle layout of the instrument. In order to separate the mechanical systems from the optical labyrinth, the periscope has been divided in a mechanical and an optical layer. The mechanical layer resides in the upper part of the periscope and consists of mirror 1, the shutter mechanism and the replacement system. The optical layer resides in the lower part of the periscope and consists of all optical elements except for mirror one. **Fehler! Verweisquelle konnte nicht gefunden werden.**

3. MCNP Model

The MCNP Model of the ITER CXRS port plug is a complete 3-dimensional full-scale model with a high level of geometric fidelity representing a detailed geometrical nodalization like depicted Fig 1. In order to simulate the neutron movements as exactly as possible the port plug has been modeled with the surrounding zones in detail consisting of a whole 20° sector of the reactor. The MCNP model, consisting of 2400 geometrical cells, was provided by the ITER Team Garching. Side surfaces are reflecting for simulating all of the 360° torus. Cells, encompassing the neutron source, are located in the middle of the torus with a mathematical approximation of the real plasma neutron generation rate.
The geometry of the CXRS Port Plug was modeled separately and coupled with the ITER model. Due to the complex geometry and continuous modifications of the design, an efficient and flexible method had to be deployed to alter the model with the design process accordingly. For this purpose an algorithm was developed, allowing the calculation of geometrical configuration of the mirror system in accordance to the actual location, size and orientation. The program produces new cards for the angles and coordinate of the surfaces for inclusion into the MCNP input file without changing the structure of the input file. Different parametric studies were performed to examine the effect of design variation for optimal performance as well as the effect of gaps between the outer surface of the port plug on the shielding performance of its surrounding structures. Dependent on the version of the model the CXRS Port Plug consists of 20 or 130 additional cells.

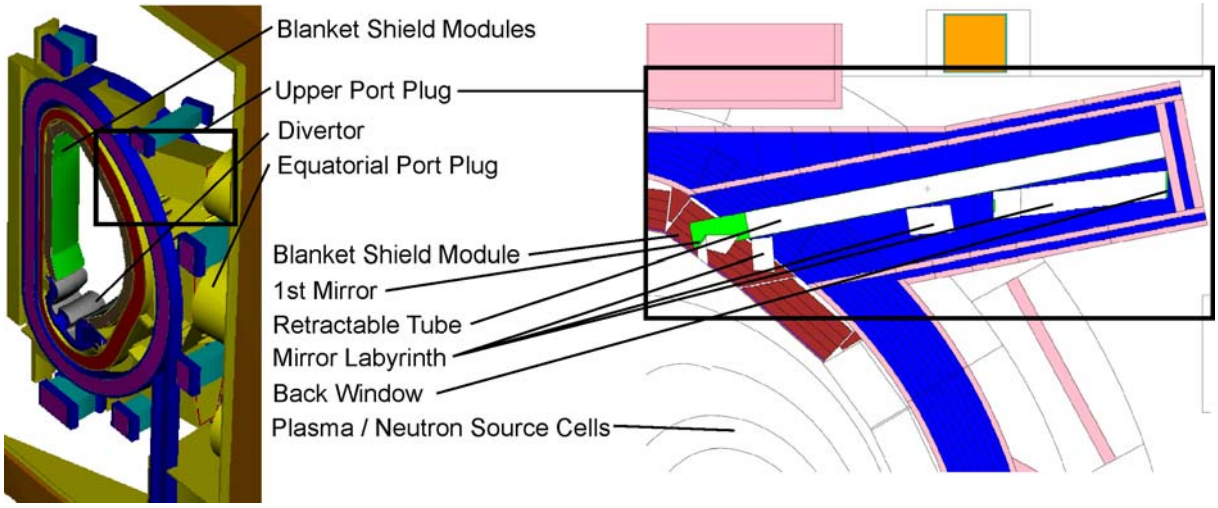

Fig 1: SABRINA plot of the MCNP model of the ITER 20° sector and a cut-away view of the CXRS Port Plug optical labyrinth with retractable tube for replacing the first mirror

Due to the shielding effects and large dimension of the model, only a small number of neutrons is tracked in the outer regions resulting in a high statistical relative errors on the calculated neutron flux. To improve the performance of the simulations, the variance reduction technique has been employed in some extend by the adjustment of cell importance. Number of neutron history was continuously increased to achieve a sufficient number of neutron tracks for a performed sampling including the outer regions of the Port Plug. The simulations have been performed on the massive-parallel computer system JUMP operated at the Research Centre Jülich.

4. Results of neutronic calculations

Due to the complexity of the geometrical model of the reactor and the large number of particle histories, the computing time was reduced significantly by the application of the parallel version of MCNP5. The simulations were carried out in steps of 1 million histories. After each step results were checked with regard to statistical errors and standard deviation and returned to MCNP by using the restart capability of the code. In total 15 Mio source particles were simulated resulting in a relative error (neutron flux) of less than 1 % around the front opening and less than 15% at the back windows of the structure. Tallies were introduced at the position of the mirrors for neutron flux and energy deposition. Additionally a row of fine mesh tallies (FMESH) was introduced to sample the areas around the mirrors, the Port Plug and ITER section. Some of the FMESH tallies were used to compute the nuclear heating by neutrons and gamma radiation in the respective material as well as the neutron damage in terms of atomic displacement. The resulting matrices were used for graphical visualization and the generation of 2D neutron flux and load patterns. A sequence of 75 matrices was combined to generate a 3D array for the neutron flux consisting of 420,000 voxels for further processing and visualization. For the verification purpose, a modified model was generated with for a former geometrical draft design of the Port Plug which was studied by a another group in the past. A comparison of the results (neutron flux and nuclear heating rate) for different mirrors in the whole port plug shows a very good agreement with the calculations reported in [4].

The calculations were performed for the new design with and without retracting tube which are compiled in Tab. 1. At the location of the first mirror in the model with retracting tube 7.30E+13 n/cm²s and 1.95 W/cm³ were calculated for neutron flux and nuclear heating respectively, representing the highest values in the Port Plug. Both values are comparable to that given in Ref. [4]. The neutron flux for the mirrors two and three is 4.53E+12 and 1.21E+13 n/cm²s respectively, showing an increase at the position of mirror three. This is due to the fact, that a higher fraction of neutrons is penetrating the shield and streaming to the position through the optical labyrinth. The nuclear heating rate at the position of mirror 2 and 3 was calculated to be 1.11E-1 and 4.00E-1 W/cm³ respectively.

	Neutron Flux [1/cm²s]		Heating [W/cm³]	
	Retractable Tube	No Retractable Tube	Retractable Tube	No Retractable Tube
Mirror 1	7.30E+13	5.56E+13	1.95E+00	1.76E+00
Mirror 2	4.53E+12	4.13E+12	1.12E-01	1.07E-01
Mirror 3	1.21E+13	1.19E+13	4.00E-01	3.88E-01
Mirror 4	4.98E+10	4.95E+10	1.40E-03	1.22E-03
Mirror 5	3.42E+09	2.90E+09	4.97E-05	4.00E-05
Mirror 6	9.33E+07	3.50E+07	9.50E-07	5.60E-07
Mirror 7	2.19E+08	7.40E+07	5.60E-06	2.88E-06
Window	4.66E+07	1.58E+07	1.20E-06	6.28E-07

Tab 1: Results of the CXRS PP neutron flux and nuclear heating calculations using MCNP

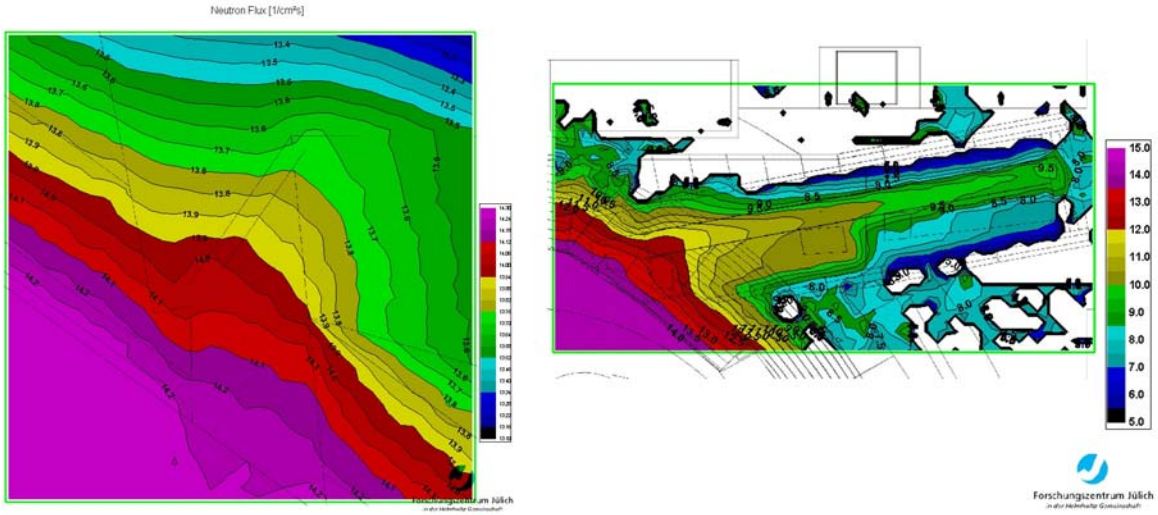

Fig 2: Results of the CXRS PP neutron flux calculations using MCNP [log(n/cm²s)] for the first mirror (left) and the whole assembly (right)

For each following mirror, the neutron flux and heating decrease rapidly due to the shielding effect of the structures. An evaluation of the calculations for the model with retractable tube shows, that the relative error for the neutron flux remains below 10% for the first five mirrors and is lower than 15% at the last two mirrors including the back window. The values at the back window are 4.66E+7 n/cm²s for the neutron flux and 1.20E-6 W/cm³ for the nuclear heating rate.

The distribution of neutron flux and heat load in the port plug system are given in Fig. 2 and Fig. 3. Left side of Fig. 2 shows the neutron flux distribution in the area around the first mirror. The values are varying inside the mirror with about one and a half order of magnitude. Visible is also the attenuation inside the materials. The right side of the Fig. 2 shows the neutron flux inside the structures of the whole Port Plug. Accordingly the maximum neutron flux appears at the rear part at the position of the retractable tube, which is modelled as a hollow cylinder to apply the worst case. The neutron flux at the window is about one order of magnitude lower. The comparison with the first configuration (with retractable tube) reveals that the use of a tube leads to significant effects to the flux at the back window. Fig. 3 displays the distribution of the neutron heating rate in the material zones. For the empty zones like the optical labyrinth and the retractable tube no values for the heating rate are displayed.

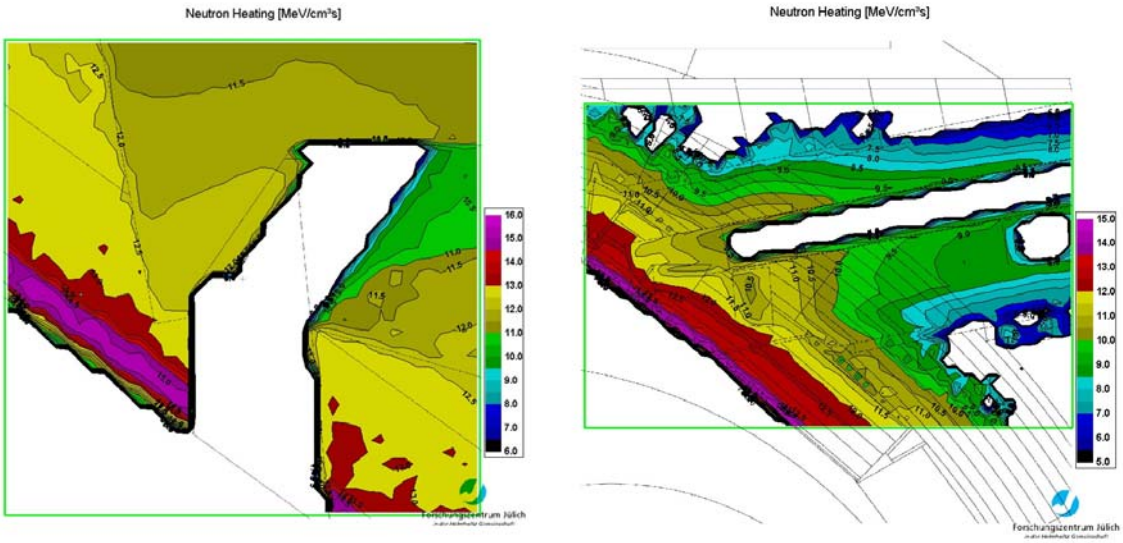

Fig 3: Results of the CXRS PP neutron heating calculations using MCNP [log(n/cm²s)] for the first mirror (left) and the whole assembly (right)

Additionally a model was created with gaps of different size around the port plug to account for streaming effect maybe caused by thermo mechanical stress. The calculation demonstrates, that gap size up to 2.5 mm only produces negligible effect on the neutron flux and heating at the rear structures and window, resulting from the shielding influence of the existing structures.

6. Conclusions

The work has shown that it is possible to calculate neutron flux and energy deposition in the whole Port Plug with sufficient precision. It is also shown, that MCNP models can be modified easily with existing tools to support frequent design modifications and parameter studies. Furthermore the presence of small gaps due to thermal expansion up to 2,5 mm are negligible because of the shielding effect of surrounding structures.

7. References

[1] Costley, A.E., et al: The Challenge of ITER Diagnostics, ECA Vol. 25A (2001) 1333-1336

[2] Briesmeister, J.F.: MCNP 4A Monte Carlo N-Particle Transport Code System, RSICC, Los Alamos, 1994, CCC-0200

[3] Di Maio, M.; Et Al.: ITER CORE CXRS Project, 2nd Intermediate Report, ITER-CXRS-CORE-FZJ-ESR-002-i1, Jülich 2007

[4] Shatalov G.E., Sheludikov, S.V.: Upper Port #3 Neutronic Analysis, Moscow 2002, Ref No. G55 MD 161 03-10-06 W 0.1.